Numer. Math. Theor. Meth. Appl.
doi: 10.4208/nmtma.OA-2023-0071

Vol. **17**, No. 1, pp. 210-242
February 2024

Divergence-Free Virtual Element Method for the Stokes Equations with Damping on Polygonal Meshes

Yu Xiong[1], Yanping Chen[3,*], Jianwei Zhou[2] and Qin Liang[1]

[1] *School of Mathematics and Computational Science, Hunan Key Laboratory for Computation and Simulation in Science and Engineering, Xiangtan University, Xiangtan 411105, P.R. China*
[2] *School of Mathematics and Statistics Linyi University, Linyi 276005, P.R. China*
[3] *School of Mathematical Sciences, South China Normal University, Guangzhou 510631, P.R. China*

Received 7 June 2023; Accepted (in revised version) 28 October 2023

Abstract. In this paper, we construct, analyze, and numerically validate a family of divergence-free virtual elements for Stokes equations with nonlinear damping on polygonal meshes. The virtual element method is $\mathbf{H}^1$-conforming and exact divergence-free. By virtue of these properties and the topological degree argument, we rigorously prove the well-posedness of the proposed discrete scheme. The convergence analysis is carried out, which imply that the error estimate for the velocity in energy norm does not explicitly depend on the pressure. Numerical experiments on various polygonal meshes validate the accuracy of the theoretical analysis and the asymptotic pressure robustness of the proposed scheme.

AMS subject classifications: 65N15, 35R05, 65N30

Key words: Optimal error estimates, divergence-free, virtual element, nonlinear damping term.

1. Introduction

In the past years, there has been a growing emphasis on studying the Stokes equations with damping due to their widespread applications in fluid mechanics, geophysics, and ocean acoustics [2, 31, 39]. In this paper, we investigate the steady Stokes equations with damping in a polygonal domain $\Omega \subset \mathbb{R}^2$ subject to homogeneous Dirichlet boundary conditions: Find a pair $(\mathbf{u}, p)$ such that

*Corresponding author. *Email addresses:* xtuyuriyxiong@gmail.com (Y. Xiong), liangqin1997@xtu.edu.cn (Q. Liang), jwzhou@yahoo.com (J. Zhou), yanpingchen@scnu.edu.cn (Y. Chen)

$$\begin{cases} -\nu\Delta\mathbf{u} + \alpha|\mathbf{u}|^{r-2}\mathbf{u} + \nabla p = \mathbf{f} & \text{in } \Omega, \\ \text{div } \mathbf{u} = 0 & \text{in } \Omega, \\ \mathbf{u} = 0 & \text{on } \partial\Omega, \end{cases} \tag{1.1}$$

where $\mathbf{u} = (u_1, u_2)$, p and $\mathbf{f}$ represent the fluid velocity, pressure and external force, respectively, $\nu > 0$ is the viscosity coefficient, $2 < r < \infty$ and $\alpha > 0$ are two damping parameters, and $|\cdot|$ denotes the Euclidean norm, i.e. $|\mathbf{u}| = \sqrt{\mathbf{u}\cdot\mathbf{u}}$. The damping term arises due to its hindering effect on fluid motion and plays a crucial role in characterizing various physical properties of the fluid, such as flow within porous media, resistance near the Earth's surface in atmospheric flows, friction effects, and other dissipative mechanisms [6, 16, 31, 32].

Over the past few decades, numerous academics have investigated and developed theoretical analyses of partial differential equations (PDEs) with damping terms. For nonlinear hyperbolic problems, the presence of the damping term $\alpha|\mathbf{u}|^{r-2}\mathbf{u}$ may result in blow-up of solution within a finite time [31, 48]. Therefore, it is imperative to conduct rigorous theoretical analyses and extensive simulation experiments to ascertain the critical value and parameter range of the damping term. For fluid problems, Constantin and Ramos [16] conducted an investigation into the long-time behavior of solutions to the two-dimensional Navier-Stokes equations with a linear damping term $\alpha\mathbf{u}$ as the viscosity coefficient approaches zero. Cai *et al.* [8, 9] delved into the long-time behavior of solutions to the Navier-Stokes equations with nonlinear damping terms, and examining the existence of global weak solutions and strong solutions.

On the numerical level, several methods have been developed for solving the Stokes equations with damping term (1.1). Liu and Li [38] proposed and analyzed the mixed finite element method for the Eqs. (1.1), and proved the well-posedness and error estimates of the proposed scheme. In [47], the weak Galerkin method combined with the two-level method were considered for the Stokes equations with damping term on general meshes and optimal error estimates of velocity and pressure were obtained. Then, by using the interior penalty discontinuous Galerkin (IPDG) method, Zhang *et al.* [57] proved the consistency and stabilization of the numerical schemes for the Eqs. (1.1) and established the error estimation of k-order of the DG-norm for velocity and L^2-norm for pressure. As highlighted in [12, 14], applying the standard finite element method to solve the such systems often leads to inaccurate and poor numerical solutions, that is, the accuracy of the approximate velocity depends on the pressure. Therefore, in order to surmount this problem or eliminate the influence of pressure on error estimates for the velocity, many scholars have done a lot of research and proposed some feasible and effective algorithms, such as the grad-div stabilization method [34, 45, 46], the pressure-robustness method [29, 37, 52], and the divergence-free method [12, 24, 58] to be utilized below.

On the other hand, most of the numerical methods for solving the Stokes equations with damping use triangular (simplicial) and quadrilateral meshes. However, with the fact that in regions of high curvature, the utilization of highly-stretched triangular or

quadrilateral elements may result in element self-intersection, causing numerical instability and inaccuracies in the solution. To address the aforementioned challenges and ensure the stabilization of the numerical method, extensive mesh refinement is often necessary. Hence, a natural idea is to use polygonal or polyhedral meshes which provide new flexibility in domain discretization and improved mesh adaptivity, especially in complex geometry [49]. The extension of conforming finite element method (FEM) to general meshes with polygonal elements is far from straightforward, because of the intricacies of constructing basis functions and the elevated computational costs associated with Gaussian integration evaluations. In the recent years, the numerical methods allowing for arbitrary-order discretizations and general meshes have significantly developed [10, 15, 17]. The virtual element method used in this article also belongs to the category of (conforming) polytopal element method.

The virtual element method (VEM) was initially proposed by Beirão da Veiga *et al.* [17,20] as an alternative way of looking at mimetic finite differences for the numerical approximation of the PDEs. The virtual element space is constructed by a polynomial subspace and the remaining non-polynomial virtual subspace. Non-polynomial components of the discrete bilinear forms are approximated using appropriate projection operators, which can be computed solely from the degrees of freedom associated with the virtual element space. Consequently, we can effectively handle meshes with more general polygonal elements, avoiding the direct computation of non-polynomial functions. Another crucial property of VEM is that the space of the basic functions is associated with the PDE problem inside the element, thus it is convenient to define divergence-free or rotation-free virtual elements [18]. For a thorough description of the VEM, see [3, 19, 41]. The (divergence-free) VEM are used to discretize the Stokes problem [12,24,29,40,42], the Brinkman problem [33,44,51], the Navier-Stokes problem [25, 56] and so on [21, 28, 30, 43, 53]. So far, we have not found any literature on divergence-free VEM for the Stokes equations with a nonlinear damping term, which constitutes another motivating and innovative aspect of this paper.

In this paper, we shall apply a Stokes-like virtual element [21, 24] for the Stokes equations with nonlinear damping term (1.1), where the method is exact divergence-free and $\mathbf{H}^1$-conforming (for the velocity). By projecting the variables in the local trilinear form onto the polynomial space of degree k using L^2 projection operator $\Pi_k^{0,E}$, we effectively address the challenges posed by the nonlinear damping term. With help of divergence-free properties and the topological degree argument described in [27], we rigorously prove the existence of the solution for the numerical scheme and provide an upper bound for it. Thus, the uniqueness of the VEM solution can be directly established. Several nonlinear analysis techniques are employed to derive the error estimation of k-order of the energy norm for velocity and L^2-norm for pressure. It should be emphasized that the velocity error does not explicitly depend on the pressure, but only indirectly through the approximation of the nonlinear damping term and the loading terms. The numerical examples on several different polyhedral meshes validated the theoretical analysis. Additionally, we conducted an analysis of the impact of the damping coefficient and the viscosity coefficient on the algorithm's solution.

The remainder of this paper is summarized as follows. Section 2 introduces the divergence-free space to transform the variational formulation of problem (1.1) into an equivalent divergence-free problem. In Section 3, we describe the detailed discretization process of the virtual element method. This leads to the formulation of the discrete divergence-free virtual element problem. Section 4 is dedicated to establishing the well-posedness of the discrete divergence-free virtual element problem. In Section 5, we derive the optimal error estimates for velocity and pressure. Finally, we present four numerical examples to validate the theoretical analysis. We also investigate the effects of the viscosity and damping coefficients in Section 6.

2. The continuous Stokes equations with damping

First of all, we will introduce some fundamental notations and function spaces. Let $\Omega \in \mathbb{R}^2$ be a convex, polygonal domain with Lipschitz boundary $\partial\Omega$. For any open subset $\omega \subseteq \Omega$, we use the standard Lebesgue space $L^p(\omega), 1 \leq p \leq \infty$ with norm $\|\cdot\|_{L^p(\omega)}$, and denote the $L^2(\omega)$ inner product by $(\cdot,\cdot)_\omega$. Let $W^{k,p}(\omega), k \geq 0$ be the k-th order of Sobolev space based on $L^p(\omega)$ and $H^k(\omega) := W^{k,2}(\omega)$, along with the corresponding norm $\|\cdot\|_{W^{k,p}(\omega)}$ and $\|\cdot\|_{H^k(\omega)}$, respectively. Set

$$H_0^1(\omega) := \left\{ v \in H^1(\omega) : v|_{\partial\omega} = 0 \right\}.$$

We denote, as usual, $H^{-1}(\omega)$ the dual space of $H_0^1(\omega)$ equipped with the dual norm $\|\cdot\|_{-1}$. Then we consider the spaces

$$\mathbf{V} := \left[H_0^1(\Omega)\right]^2, \quad Q := L_0^2(\Omega) = \left\{ q \in L^2(\Omega) \text{ such that } \int_\Omega q \, d\Omega = 0 \right\}$$

with norms

$$\|\mathbf{v}\|_{\mathbf{V}} := \|\nabla \mathbf{v}\|_0 = |\mathbf{v}|_1, \quad \|q\|_Q := \|q\|_{L^2(\Omega)}. \tag{2.1}$$

Having these, the weak formulation of (1.1) is to find a pair $(\mathbf{u}, p) \in \mathbf{V} \times Q$ such that

$$\begin{cases} \nu\, a(\mathbf{u},\mathbf{v}) + \alpha\, c(\mathbf{u};\mathbf{u},\mathbf{v}) + b(\mathbf{v},q) = (\mathbf{f},\mathbf{v}), & \forall \mathbf{v} \in \mathbf{V}, \\ b(\mathbf{u},q) = 0, & \forall q \in Q, \end{cases} \tag{2.2}$$

where the source item $\mathbf{f} \in [L^2(\Omega)]^2$, and consider the following linear forms:

$$a(\cdot,\cdot): \quad \mathbf{V}\times\mathbf{V} \to \mathbb{R}, \qquad a(\mathbf{u},\mathbf{v}) := \int_\Omega \nabla\mathbf{u} : \nabla\mathbf{v}\, d\Omega, \qquad \forall \mathbf{u},\mathbf{v} \in \mathbf{V}, \tag{2.3}$$

$$c(\cdot;\cdot,\cdot): \ \mathbf{V}\times\mathbf{V}\times\mathbf{V} \to \mathbb{R}, \quad c(\mathbf{w};\mathbf{u},\mathbf{v}) := \int_\Omega |\mathbf{w}|^{r-2}\, \mathbf{u}\, \mathbf{v}\, d\Omega, \ \forall \mathbf{w},\mathbf{u},\mathbf{v} \in \mathbf{V}, \tag{2.4}$$

$$b(\cdot,\cdot): \quad \mathbf{V}\times Q \to \mathbb{R}, \qquad b(\mathbf{v},q) := -\int_\Omega p \ \mathrm{div}\ \mathbf{v}\, d\Omega, \qquad \forall \mathbf{v} \in \mathbf{V}, \quad q \in Q, \tag{2.5}$$

and

$$(\mathbf{f}, \mathbf{v}) := \int_{\Omega} \mathbf{f} \cdot \mathbf{v} \, d\,\Omega. \tag{2.6}$$

By employing a topological degree argument (as presented in [26]) and nonlinear functional analysis techniques, we can easily prove the well-posedness of the solution for the weak formulation (2.2).

Theorem 2.1. *We assume that* $\mathbf{f} \in [H^{-1}(\Omega)]^2$ *and that* $\nu \in L^{\infty}(\Omega)$ *is a uniformly positive constant in* Ω*. There exits a solution* $(\mathbf{u}, p) \in \mathbf{V} \times Q$ *of weak formulation* (2.2) *satisfying the following estimates:*

$$\|\mathbf{u}\|_{\mathbf{V}} \leq \frac{\|\mathbf{f}\|_{-1}}{\nu}, \tag{2.7}$$

where

$$\|\mathbf{f}\|_{-1} = \|\mathbf{f}\|_{\mathbf{V}'} := \sup_{\mathbf{v} \in \mathbf{V}} \frac{(\mathbf{f}, \mathbf{v})}{\|\mathbf{v}\|_{\mathbf{V}}}.$$

The proof of the uniqueness for the solution $(\mathbf{u}, p) \in \mathbf{V} \times Q$ is straightforward.

Throughout the remainder of the paper, C represents a positive constant that may assume varying values in different contexts. Additionally, we will employ the following assumption in our subsequent proof:

$$\gamma := \frac{\|\mathbf{f}\|_{-1}}{\nu} < C. \tag{2.8}$$

Let $\mathbf{Z}$ denote the divergence-free subspace of $\mathbf{V}$, defined as the following:

$$\mathbf{Z} := \big\{ \mathbf{v} \in \mathbf{V} \ \text{ such that } \ b(\mathbf{v}, q) = 0 \ \forall q \in Q \big\}. \tag{2.9}$$

Then the problem (2.2) can be reformulated as the equivalent divergence-free problem: Find $\mathbf{u} \in \mathbf{Z}$ such that

$$\nu \, a(\mathbf{u}, \mathbf{v}) + \alpha \, c(\mathbf{u}; \mathbf{u}, \mathbf{v}) = (\mathbf{f}, \mathbf{v}), \quad \forall \mathbf{v} \in \mathbf{Z}. \tag{2.10}$$

3. Virtual element discretization

In this section, we develop the divergence-free virtual element formulation for the model problem (2.2). To achieve this, we first introduce the concept of polygonal subdivision of Ω and the virtual element spaces in Subsection 3.1. Subsequently, in Subsection 3.2, we introduce the discrete bilinear forms in the virtual element spaces. With these preparations, we derive a discrete divergence-free virtual element problem in Subsection 3.3.

3.1. Virtual element spaces and polynomial projections

Let $\{\Omega_h\}$ represent the sequence of Ω subdivided into a set of general polygonal elements E with

$$h_E := \text{diameter}(E), \quad h := \sup_{E\in\Omega_h} h_E.$$

As mentioned in [7], there are certain restrictions on the polygon E.

Assumption 3.1. There exists a positive real number ρ such that for all h and for every $E \in \Omega_h$

- the ratio between the shortest edge $e_{\min}$ and the diameter h_E of E is greater than ρ, i.e.,
$$\frac{e_{\min}}{h_E} > \rho,$$
- E is star-shaped with respect to a ball of radius ρh_E.

We note that the assumptions above are common and can be further relaxed, as discussed in [23]. Here, we provide a remark about the star-shaped region.

Remark 3.1. We refer to the domain $\Omega \subset \mathbb{R}^2$ as star-shaped with respect to a circle B (referred to as a ball in $\mathbb{R}^3$) if, for all $x \in \Omega$, the closed convex hull of $x \cup B$ is still a subset of Ω. In Fig. 1(a), Ω_1 is star-shaped with respect to circle B_1, while with respect to B_2, it is not. In Fig. 1(b), Ω_2 is not star-shaped with respect to any circle.

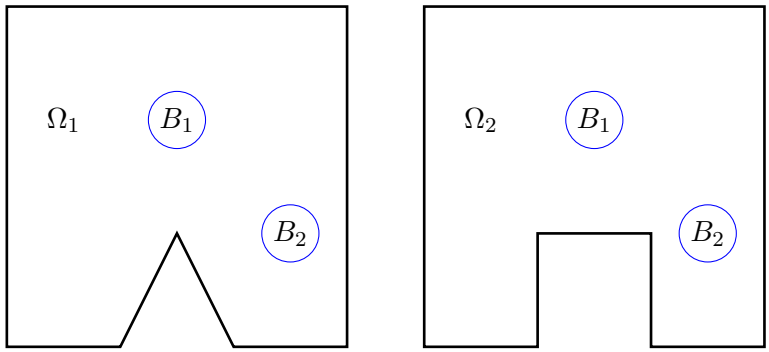

Figure 1: (a) Ω_1 is star-shaped; (b) Ω_2 is not star-shaped.

Following [24], we introduce some well-known virtual element spaces for the Stokes problem on polygonal meshes. For any $k \in \mathbb{N}$, we define the spaces as follows:

- $\mathbb{P}_k(E)$ denotes a set of polynomials on E of degree $\leq k$,
- $\mathbb{B}_k(\partial E) := \{\mathbf{v} \in C^0(\partial E) \text{ such that } \mathbf{v}|_e \in \mathbb{P}_k(e), \ \forall e \subset \partial E\}$,
- $\mathcal{G}_k(E) := \nabla(\mathbb{P}_{k+1}(E)) \subseteq [\mathbb{P}_k(E)]^2$,
- $\mathcal{G}_k^{\oplus}(E) := \mathbf{x}^{\perp}[\mathbb{P}_{k-1}(E)] \subseteq [\mathbb{P}_k(E)]^2$ is defined as the L^2-orthogonal complement to $\mathcal{G}_k(E)$, where $\mathbf{x}^{\perp} := (x_2, -x_1)$.

For a geometric domain $\mathcal{D}$ of dimension d $(d = 1, 2)$, as an edge or an element, let $\mathbf{x}_{\mathcal{D}}$ and $h_{\mathcal{D}}$ be the barycenter and the diameter of $\mathcal{D}$, respectively. We denote by $\mathcal{M}_k(\mathcal{D})$ the scaled monomial set as the basis for the polynomial space $\mathbb{P}_k(\mathcal{D})$ defined on $\mathcal{D}$ [1, 17, 20]. Define $\mathcal{M}_k(\mathcal{D})$ as the set of scaled monomials with degrees less than or equal to k

$$\mathcal{M}_k(\mathcal{D}) := \left\{ m \mid m = \left(\frac{\mathbf{x} - \mathbf{x}_{\mathcal{D}}}{h_{\mathcal{D}}} \right)^{\alpha} \text{ for } \alpha \in \mathbb{N}^d,\ 0 \le |\alpha| \le k \right\}.$$

Remark 3.2. As a basis for the polynomial space $\mathbb{P}_k(\mathcal{D})$, the set of scaled monomials $\mathcal{M}_k(\mathcal{D})$ offering adaptability to various complicated geometric conditions and mesh types. This advantage is particularly significant in specific fields, such as fluid dynamics or structural mechanics.

Then we briefly introduce the (original) finite-dimensional local virtual space [24] on each element $E \in \Omega_h$

$$\mathbf{W}_h^E := \Bigg\{ \mathbf{v} \in \left[H^1(E)\right]^2 \text{ such that } \mathbf{v}_{|\partial E} \in [\mathbb{B}_k(\partial E)]^2 \text{ and } -\boldsymbol{\Delta}\mathbf{v} - \nabla s \in \mathcal{G}_{k-2}^{\oplus}(E), \\ \operatorname{div} \mathbf{v} \in \mathbb{P}_{k-1}(E) \text{ for an } s \in L^2(E) \Bigg\}. \tag{3.1}$$

It is worth mentioning that all operators and equations presented above should be interpreted in the distributional sense. Obviously, we notice that $[\mathbb{P}_k(E)]^2 \subseteq \mathbf{W}_h^E$. And the global original virtual element space defined as

$$\mathbf{W}_h := \left\{ \mathbf{v} \in \left[H_0^1(\Omega)\right]^2 \text{ such that } \mathbf{v}_{|E} \in \mathbf{W}_h^E,\ \forall E \in \Omega_h \right\}.$$

For the sake of simplicity, we define the degrees of freedom (DoFs) in the local space $\mathbf{W}_h^E$. For a function $\mathbf{v} \in \mathbf{W}_h^E$, we determine its corresponding DoFs by specifying the linear operators $\mathbf{D_V}$, which are divided into four distinct subsets as illustrated in Fig. 2:

$\mathbf{D_V}1$. The values of $\mathbf{v}$ at the vertices of polygon E.

$\mathbf{D_V}2$. The values of $\mathbf{v}$ at $k-1$ distinct points on every edge $e \in \partial E$ (for example, we can use the $k-1$ internal points of the $(k+1)$-Gauss-Lobatto quadrature rule on e, as recommended in [20]).

$\mathbf{D_V}3$. The moments of $\mathbf{v}$,

$$\int_E \mathbf{v} \cdot g_{k-2}^{\oplus}(E)\, \mathrm{d}\mathbf{x} \quad \text{for all} \quad g_{k-2}^{\oplus}(E) \in \mathcal{G}_{k-2}^{\oplus}(E).$$

$\mathbf{D_V}4$. The moments up to order $k-1$ for $k > 1$ of $\operatorname{div} \mathbf{v}$, i.e.

$$\int_E (\operatorname{div} \mathbf{v}) q_{k-1}\, \mathrm{d}\mathbf{x} \quad \text{for all} \quad q_{k-1} \in \mathbb{P}_{k-1}(E)/\mathbb{R}.$$

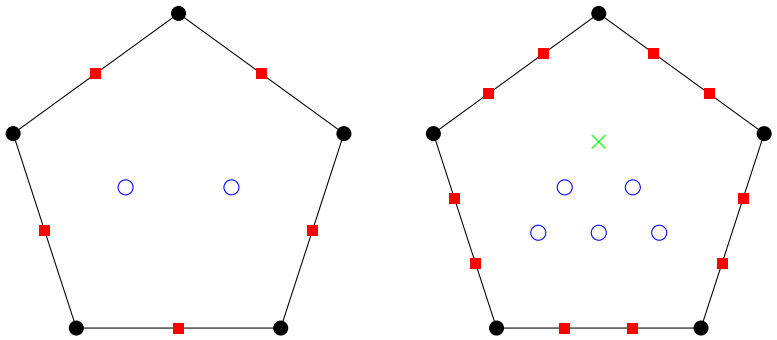

(a) (b)

Figure 2: Degrees of freedom. (a) $k = 2$. (b) $k = 3$. We represent $\mathbf{D_V}1$ with the black dots, $\mathbf{D_V}2$ with the red squares, $\mathbf{D_V}3$ with the green cross, $\mathbf{D_V}4$ with the blue circles.

Proposition 3.1 ([24]). *The linear operators $\mathbf{D_V}$ constitute a unisolvent set of DoFs for the virtual space $\mathbf{W}_h^E$.*

Next, we introduce the $\boldsymbol{H}^1$ seminorm projection operator $\Pi_k^{\nabla,E}$ and the L^2 projection operator $\Pi_k^{0,E}$ for all $E \in \Omega_h$ and $k \in \mathbb{N}$ as follows:

- The $\boldsymbol{H}^1$ seminorm projection operator $\Pi_k^{\nabla,E} : \mathbf{V} \to [\mathbb{P}_k(E)]^2$,

$$\begin{cases} \displaystyle\int_E \nabla \mathbf{q}_k : \boldsymbol{\nabla}\left(\mathbf{v} - \Pi_k^{\nabla,E}\mathbf{v}\right) \,\mathrm{d}\mathbf{x} = 0, \quad \forall \mathbf{v} \in \mathbf{V}, \quad \forall \mathbf{q}_k \in [\mathbb{P}_k(E)]^2, \\ \displaystyle\int_{\partial E} \mathbf{q}_0 \cdot \left(\mathbf{v} - \Pi_k^{\nabla,E}\mathbf{v}\right) \mathrm{d}s = 0, \qquad \forall \mathbf{v} \in \mathbf{V}, \quad \forall \mathbf{q}_0 \in [\mathbb{P}_0(E)]^2. \end{cases} \tag{3.2}$$

- The L^2 projection operator for scalar functions $\Pi_k^{0,E} : L^2(E) \to \mathbb{P}_k(E)$,

$$\int_E q_k \left(v - \Pi_k^{0,E} v\right) \,\mathrm{d}\mathbf{x} = 0, \quad \forall v \in L^2(E), \quad \forall q_k \in \mathbb{P}_n(E). \tag{3.3}$$

Additionally, it is obvious that the $\boldsymbol{L}^2$ projection operator can be extended to vector functions

$$\Pi_k^{0,E} : \left[L^2(\Omega)\right]^2 \to [\mathbb{P}_k(E)]^2, \quad \boldsymbol{\Pi}_k^{0,E} : \left[L^2(E)\right]^{2\times 2} \to [\mathbb{P}_k(E)]^{2\times 2}.$$

It is worth noting that the positive integer $k \geq 2$ represents the polynomial degree of accuracy in the virtual element method. We can confirm that the DoFs enable accurate calculation of the L^2 projection operator $\Pi_{k-2}^{0,E} : \mathbf{W}_h^E \to [\mathbb{P}_{k-2}(E)]^2$, as demonstrated in [24, Section 3.3]. Nonetheless, we have observed that accurate calculation of the L^2 projection cannot be achieved using the DoFs on polynomial spaces of degree $k-1$ and k. Inspired by [1], we introduce the modified local virtual element space for the discrete problem.

First of all, we introduce the enlarged (also called augmented) virtual local space $\mathbf{U}_h^E$,

$$\mathbf{U}_h^E := \Bigg\{ \mathbf{v} \in \left[H^1(E)\right]^2 \text{ such that } \mathbf{v}_{|\partial E} \in [\mathbb{B}_k(\partial E)]^2 \text{ and } -\boldsymbol{\Delta}\mathbf{v} - \nabla s \in \mathcal{G}_k^{\oplus}(E), \\ \operatorname{div}\mathbf{v} \in \mathbb{P}_{k-1}(E) \text{ for an } s \in L^2(E) \Bigg\}. \tag{3.4}$$

Next, we define the modified virtual element space $\mathbf{V}_h^E$, by restricting $\mathbf{U}_h^E$ to a subspace

$$\mathbf{V}_h^E := \Bigg\{ \mathbf{v} \in \mathbf{U}_h^E \text{ such that } \left(\mathbf{v} - \Pi_k^{\nabla,E}\mathbf{v}, \mathbf{g}_k^{\perp}\right)_{[L^2(E)]^2} = 0, \\ \forall\, \mathbf{g}_k^{\perp} \in \mathcal{G}_k^{\oplus}(E)/\mathcal{G}_{k-2}^{\oplus}(E) \Bigg\}, \tag{3.5}$$

where $\mathcal{G}_k^{\oplus}(E)/\mathcal{G}_{k-2}^{\oplus}(E)$ represents the subset of polynomials in $\mathcal{G}_k^{\oplus}(E)$ that are L^2-orthogonal to all polynomials in $\mathcal{G}_{k-2}^{\oplus}(E)$. Clearly, the dimension of the modified space $\mathbf{V}_h^E$ is equal to that of the original space $\mathbf{W}_h^E$.

Proposition 3.2 (Projections and Computability)**.** *The DoFs* $\mathbf{D_V}$ *enable us to compute exactly*

$$\Pi_{\mathrm{k}}^{\nabla,\mathrm{E}} : \mathbf{V}_h^E \to [\mathbb{P}_k(E)]^2, \quad \Pi_{\mathrm{k}}^{0,\mathrm{E}} : \mathbf{V}_h^E \to [\mathbb{P}_k(E)]^2, \quad \boldsymbol{\Pi}_{\mathrm{k-1}}^{0,\mathrm{E}} : \boldsymbol{\nabla}\left(\mathbf{V}_h^E\right) \to [\mathbb{P}_{k-1}(E)]^{2\times 2}$$

in the sense that, for all $\mathbf{v}_h \in \mathbf{V}_h^E$*, we can compute the polynomials* $\Pi_{\mathrm{k}}^{\nabla,\mathrm{E}}\mathbf{v}_h$*,* $\Pi_{\mathrm{k}}^{0,\mathrm{E}}\mathbf{v}_h$ *and* $\boldsymbol{\Pi}_{\mathrm{k-1}}^{0,\mathrm{E}}\mathbf{v}_h$ *solely based on the DoFs values* $\mathbf{D_V}$ *of* $\mathbf{v}_h$*.*

Furthermore, for any polynomial q_n of arbitrary degree n and any $\mathbf{v} \in \mathbf{V}_h^E$, integration by parts allows us to calculate the moment

$$\int_E \nabla q_n \cdot \mathbf{v}\, \mathrm{d}\mathbf{x} = \int_{\partial E} q_n \mathbf{v}\cdot\mathbf{n}\, \mathrm{d}S - \int_E q_n\, \operatorname{div}\mathbf{v}\, \mathrm{d}\mathbf{x}.$$

Concerning the pressure, we utilize the standard finite-dimensional polynomial space denoted as

$$Q_h^E := \mathbb{P}_{k-1}(E) \tag{3.6}$$

with a dimension

$$\dim\left(Q_h^E\right) = \dim\left(\mathbb{P}_{k-1}(E)\right) = \frac{(k+1)k}{2}.$$

For each $q \in Q_h^E$, we introduce related DoFs with the linear operators $\mathbf{D_Q}$ defined as the moments up to $k-1$ of q, i.e.,

$$\int_E q p_{k-1} \mathrm{d}\mathbf{x} \quad \text{for all} \quad p_{k-1} \in \mathbb{P}_{k-1}(E).$$

Finally, the global virtual element spaces is defined as

$$\mathbf{V}_h := \left\{ \mathbf{v} \in \left[H_0^1(\Omega)\right]^2 \text{ such that } \mathbf{v}|_E \in \mathbf{V}_h^E,\ \forall E \in \Omega_h \right\}, \tag{3.7}$$

$$Q_h := \left\{ q \in L_0^2(\Omega) \text{ such that } q|_E \in Q_h^E,\ \forall E \in \Omega_h \right\} \tag{3.8}$$

with the obvious corresponding sets of global DoFs. It is easy for us to compute the dimension of $\mathbf{V}_h$ and Q_h

$$\dim(\mathbf{V}_h) = n_P \left(\frac{(k+1)k}{2} - 1 + \frac{(k-1)(k-2)}{2} \right) + 2\big(n_V + (k-1)n_e\big),$$

and

$$\dim(Q_h) = n_P \frac{(k+1)k}{2} - 1,$$

where n_P denotes the number of elements, while n_e and n_V represent the count of internal edges and vertices in Ω_h, respectively. As noted in [24], it is noteworthy that

$$\operatorname{div} \mathbf{V}_h \subseteq Q_h. \tag{3.9}$$

3.2. Discretization of linear form

Firstly, we decompose the bilinear forms $a(\cdot,\cdot)$ and $b(\cdot,\cdot)$, the trilinear form $c(\cdot;\cdot,\cdot)$, as well as the norms $|\cdot|_{\mathbf{V}}$ and $|\cdot|_Q$ into local contributions through the following definitions:

$$\begin{aligned}
a(\mathbf{u},\mathbf{v}) &:= \sum_{E\in\Omega_h} a^E(\mathbf{u},\mathbf{v}) && \text{for all} \quad \mathbf{u},\mathbf{v} \in \mathbf{V},\\
b(\mathbf{v},q) &:= \sum_{E\in\Omega_h} b^E(\mathbf{v},q) && \text{for all} \quad \mathbf{v} \in \mathbf{V} \quad \text{and} \quad q \in Q,\\
c(\mathbf{w};\mathbf{u},\mathbf{v}) &:= \sum_{E\in\Omega_h} c^E(\mathbf{w};\mathbf{u},\mathbf{v}) && \text{for all} \quad \mathbf{w},\mathbf{u},\mathbf{v} \in \mathbf{V}
\end{aligned}$$

with broken norm

$$\begin{aligned}
\|\mathbf{v}\|_{\mathbf{V}} &:= \left(\sum_{E\in\Omega_h} \|\mathbf{v}\|_{\mathbf{V},E}^2 \right)^{\frac{1}{2}} && \text{for all} \quad \mathbf{v} \in \mathbf{V},\\
\|q\|_Q &:= \left(\sum_{E\in\Omega_h} \|q\|_{Q,E}^2 \right)^{\frac{1}{2}} && \text{for all} \quad q \in Q.
\end{aligned}$$

Then we give the discretization of linear form. Concerning $b(\cdot,\cdot)$, we have

$$b(\mathbf{v},q) = \sum_{E\in\Omega_h} b^E(\mathbf{v},q) = \sum_{E\in\Omega_h} \int_E \operatorname{div}\mathbf{v} q \,\mathrm{d}\mathbf{x} \quad \text{for all} \quad \mathbf{v} \in \mathbf{V}_h, \quad q \in Q_h. \tag{3.10}$$

Therefore, there is no need to introduce any approximations of $b(\cdot,\cdot)$, as mentioned in [24], since q can be expressed as a scale polynomial in each element $E \in \Omega_h$. Obviously, (3.10) can be exactly computed from the DoFs.

We observe that the quantities $a^E(\mathbf{u},\mathbf{v})$ and $c^E(\mathbf{w},\mathbf{u},\mathbf{v})$ are uncomputable for an arbitrary $(\mathbf{w},\mathbf{u},\mathbf{v}) \in \mathbf{V}_h^E \times \mathbf{V}_h^E \times \mathbf{V}_h^E$. Therefore, following a standard procedure within the VEM framework, we introduce computable discrete local forms $a_h^E(\cdot,\cdot)$ and $c_h^E(\cdot;\cdot,\cdot)$ as approximations to the continuous form $a^E(\cdot,\cdot)$ and $c^E(\cdot;\cdot,\cdot)$, respectively. For all $(\mathbf{w},\mathbf{u},\mathbf{v}) \in \mathbf{V}_h^E \times \mathbf{V}_h^E \times \mathbf{V}_h^E$, we define

$$a_h^E(\mathbf{u},\mathbf{v}) := a^E\left(\Pi_{\mathrm{k}}^{\nabla,\mathrm{E}}\mathbf{u}, \Pi_{\mathrm{k}}^{\nabla,\mathrm{E}}\mathbf{v}\right) + \mathcal{S}^E\left(\left(I-\Pi_{\mathrm{k}}^{\nabla,\mathrm{E}}\right)\mathbf{u}, \left(I-\Pi_{\mathrm{k}}^{\nabla,\mathrm{E}}\right)\mathbf{v}\right), \tag{3.11}$$

$$c_h^E(\mathbf{w};\mathbf{u},\mathbf{v}) := c^E\left(\Pi_k^{0,E}\mathbf{w}; \Pi_k^{0,E}\mathbf{u}, \Pi_k^{0,E}\mathbf{v}\right), \tag{3.12}$$

where the bilinear form $\mathcal{S}^E(\cdot,\cdot)$ is expected to possess continuity and coercivity on $\mathbf{V}_h^E \cap \ker(\Pi_k^{\nabla,E})$ uniformly in the mesh element. Fortunately, [42] has established a valid stability bounds: the symmetric stabilizing bilinear form $\mathcal{S}^E : \mathbf{V}_h^E \times \mathbf{V}_h^E \to \mathbb{R}$ satisfies

$$\alpha_* a^E(\mathbf{v},\mathbf{v}) \le \mathcal{S}^E(\mathbf{v},\mathbf{v}) \le \alpha^* a^E(\mathbf{v},\mathbf{v}) \tag{3.13}$$

for all $\mathbf{v} \in \mathbf{V}_h$ such that $\Pi_k^{\nabla,E}\mathbf{v} = \mathbf{0}$, where the positive constant α_* and α^* remain independent of both the element E and the mesh size h, but they are dependent on the polynomial degree k.

Proposition 3.3. *For each element $E \in \Omega_h$, the discrete local bilinear $a_h^E(\cdot,\cdot)$ satisfies the following properties:*

(i) k-Consistency: for all $\mathbf{w} \in L^2(E)$, $\mathbf{q}_k \in [\mathbb{P}_k(E)]^2$ and $\mathbf{v} \in \mathbf{V}_h^E$,

$$a_h^E(\mathbf{q}_k,\mathbf{v}) = a^E(\mathbf{q}_k,\mathbf{v}). \tag{3.14}$$

(ii) Stability: there exist two positive constants α_* and α^* (as shown in (3.13)) that are independent of h and E, such that for all $\mathbf{v} \in \mathbf{V}_h^E$, the following inequality holds:

$$\alpha_* a^E(\mathbf{v},\mathbf{v}) \le a_h^E(\mathbf{v},\mathbf{v}) \le \alpha^* a^E(\mathbf{v},\mathbf{v}). \tag{3.15}$$

Remark 3.3. In fact, we can readily verify that the definition of the projection operator (3.2) and the property (3.13) imply the consistency (3.14) and stability (3.15). The stabilization term $\mathcal{S}^E(\mathbf{v}_h,\mathbf{v}_h)$ has the same scale as $a^E(\mathbf{v}_h,\mathbf{v}_h)$. For instance, following the most standard VEM choice [17, 20, 22], the stabilization term $\mathcal{S}^E$ can defined as

$$\mathcal{S}^E(\mathbf{u}_h,\mathbf{v}_h) := \varepsilon^E \sum_{i=1}^{N_V^E} \chi_i(\mathbf{v}_h)\chi_i(\mathbf{v}_h),$$

where $N_V^E = \dim \mathbf{V}_h^E$ and $\chi_i(\mathbf{v}_h)$ denotes the i-th local DoFs on $\mathbf{V}_h^E$ and ε^E is a suitable positive constant that is dependent on E.

Subsequently, we define the bilinear form and the trilinear form of global approximation $a_h(\cdot,\cdot) : \mathbf{V}_h \times \mathbf{V}_h \to \mathbb{R}$ and $c_h(\cdot;\cdot,\cdot) : \mathbf{V}_h \times \mathbf{V}_h \times \mathbf{V}_h \to \mathbb{R}$ by simply accumulating the local contributions

$$a_h(\mathbf{u},\mathbf{v}) := \sum_{E\in\Omega_h} a_h^E(\mathbf{u},\mathbf{v}), \qquad \forall \mathbf{u},\mathbf{v} \in \mathbf{V}_h, \tag{3.16}$$

$$c_h(\mathbf{w};\mathbf{u},\mathbf{v}) := \sum_{E\in\Omega_h} c_h^E(\mathbf{w};\mathbf{u},\mathbf{v}), \quad \forall \mathbf{w},\mathbf{u},\mathbf{v} \in \mathbf{V}_h. \tag{3.17}$$

Finally, we will construct a computable approximation of the right-hand side $(\mathbf{f},\mathbf{v})$ in (2.2) by using $\Pi_k^{0,E}$ defined in (3.3). The approximated load term $\mathbf{f}_h$ is defined as follows:

$$\mathbf{f}_h := \Pi_k^{0,E}\mathbf{f} \quad \text{for all} \quad E \in \Omega_h. \tag{3.18}$$

And the associated right-hand side

$$\begin{aligned}(\mathbf{f}_h,\mathbf{v}_h) &= \sum_{E\in\Omega_h}\int_E \mathbf{f}_h\cdot\mathbf{v}_h \,\mathrm{d}\mathbf{x} \equiv \sum_{E\in\Omega_h}\int_E \Pi_{\mathrm{k}}^{0,E}\mathbf{f}\cdot\mathbf{v}_h \,\mathrm{d}\mathbf{x}\\ &= \sum_{E\in\Omega_h}\int_E \mathbf{f}\cdot\Pi_{\mathrm{k}}^{0,E}\mathbf{v}_h \,\mathrm{d}\mathbf{x}\end{aligned} \tag{3.19}$$

can be exactly computed from DoFs for all $\mathbf{v}_h \in V_h$ representing the internal moments.

3.3. The discrete problem

With these preparations completed, it is not difficult to derive the following virtual element problem: Find $(\mathbf{u}_h, p_h) \in \mathbf{V}_h \times Q_h$ such that

$$\begin{cases}\nu\, a_h(\mathbf{u}_h,\mathbf{v}_h) + \alpha\, c_h(\mathbf{u}_h;\mathbf{u}_h,\mathbf{v}_h) + b(\mathbf{v}_h,p_h) = (\mathbf{f}_h,\mathbf{v}_h) & \text{for all} \quad \mathbf{v}_h \in \mathbf{V}_h,\\ b(\mathbf{u}_h,q_h) = 0 & \text{for all} \quad q_h \in Q_h.\end{cases} \tag{3.20}$$

We define the discrete divergence-free subspace of $\mathbf{V}_h$ as follows [24]:

$$\mathbf{Z}_h := \big\{\mathbf{v}_h \in \mathbf{V}_h \ \text{ such that } \ b(\mathbf{v}_h,q_h) = 0,\ \forall q_h \in Q_h\big\}. \tag{3.21}$$

By virtue of the stability (3.15) and the inclusion $\mathbf{Z}_h \in \mathbf{V}_h$, the bilinear form $a_h(\cdot,\cdot)$ is coercive on $\mathbf{Z}_h$. From [13,24], we have the following inf-sup condition for $b(\cdot,\cdot)$: there exists a positive constant $\widehat{\beta}$, which is independent of both h and the degree of accuracy k such that

$$\sup_{\mathbf{v}_h\in\mathbf{V}_h,\mathbf{v}_h\neq\mathbf{0}} \frac{b(\mathbf{v}_h,q_h)}{\|\mathbf{v}_h\|_{\mathbf{V}}} \geq \widehat{\beta}\,\|q_h\|_Q \quad \text{for all} \quad q_h \in Q_h. \tag{3.22}$$

With help of the divergence-free space $\mathbf{Z}_h$, the virtual element problem (3.20) can be also reformulated as the equivalent divergence-free form: Find $\mathbf{u}_h \in \mathbf{Z}_h$ such that

$$\nu\, a_h(\mathbf{u}_h,\mathbf{v}_h) + \alpha\, c(\mathbf{u}_h;\mathbf{u}_h,\mathbf{v}_h) = (\mathbf{f}_h,\mathbf{v}_h) \quad \text{for all} \quad \mathbf{v}_h \in \mathbf{Z}_h. \tag{3.23}$$

Remark 3.4. The discrete divergence-free space provides a crucial property for the method, ensuring that the discrete velocity is pointwise divergence-free. This property enables the velocity error to be independent of the pressure in the convergence analysis of Section 5. In certain cases, such as hydrostatic fluid problems, the partial decoupling of errors exhibits a favorable impact on the velocity approximation.

4. Existence and uniqueness

The aim of this section is to prove that the divergence-free virtual problem (3.23) is well-posedness. To this purpose, we firstly provide the following upper bound of the trilinear form $c_h(\cdot;\cdot,\cdot)$.

Lemma 4.1. *For any $\mathbf{u},\mathbf{v},\mathbf{w}\in\mathbf{V}$, we have*

$$c_h(\mathbf{w};\mathbf{u},\mathbf{v})\leq C\|\mathbf{w}\|_{\mathbf{V}}^{r-2}\|\mathbf{u}\|_{\mathbf{V}}\|\mathbf{v}\|_{\mathbf{V}}, \tag{4.1}$$

where C is a constant independent of h but dependent on k.

Proof. Employing the continuity of the projection $\Pi_k^{0,E}$ with respect to the L^2-norm, we can readily get $\|\Pi_k^{0,E}\mathbf{u}\|_{0,E}\leq\|\mathbf{u}\|_{0,E}$. Then by using local inverse theorem and Hölder inequality in $E\in\Omega_h$, we have

$$\begin{aligned}\left\|\Pi_k^{0,E}\mathbf{u}\right\|_{L^r(E)}&\leq Ch^{\frac{2}{r}-\frac{2}{2}}\left\|\Pi_k^{0,E}\mathbf{u}\right\|_{0,E}\leq Ch^{\frac{2}{r}-\frac{2}{2}}\|\mathbf{u}\|_{0,E}\\&\leq Ch^{\frac{2}{r}-\frac{2}{2}}\|1\|_{L^{\frac{2r}{r-2}}(E)}\|\mathbf{u}\|_{L^r(E)}\\&\leq Ch^{\frac{2}{r}-\frac{2}{2}}h^{2\cdot\frac{r-2}{2r}}\|\mathbf{u}\|_{L^r(E)}\\&\leq C\|\mathbf{u}\|_{L^r(E)}.\end{aligned} \tag{4.2}$$

Throughout the remainder of the paper, we also refer to (4.2) as the continuity of the projection $\Pi_k^{0,E}$ with respect to the L^r-norm. Then, by using Hölder inequality and (4.2), we have

$$\begin{aligned}c_h^E(\mathbf{w};\mathbf{u},\mathbf{v})&:=\left(\left|\Pi_{\mathrm{k}}^{0,E}\mathbf{w}\right|^{r-2}\Pi_{\mathrm{k}}^{0,E}\mathbf{u},\Pi_{\mathrm{k}}^{0,E}\mathbf{v}\right)\\&\leq C\left(\int_E\left(\left|\Pi_k^{0,E}\mathbf{w}\right|^{r-2}\right)^{\frac{r}{r-2}}\,\mathrm{d}\mathbf{x}\right)^{\frac{r-2}{r}}\left(\int_E\left(\Pi_k^{0,E}\mathbf{u}\right)^r\,\mathrm{d}\mathbf{x}\right)^{\frac{1}{r}}\\&\quad\times\left(\int_E\left(\Pi_k^{0,E}\mathbf{v}\right)^r\,\mathrm{d}\mathbf{x}\right)^{\frac{1}{r}}\\&=C\left\|\Pi_k^{0,E}\mathbf{w}\right\|_{L^r(E)}^{r-2}\left\|\Pi_k^{0,E}\mathbf{u}\right\|_{L^r(E)}\left\|\Pi_k^{0,E}\mathbf{v}\right\|_{L^r(E)}\\&\leq C\|\mathbf{w}\|_{L^r(E)}^{r-2}\|\mathbf{u}\|_{L^r(E)}\|\mathbf{v}\|_{L^r(E)}.\end{aligned}$$

Using once again Hölder inequality and Sobolev embedding ($H^1(\Omega)\hookrightarrow L^r(\Omega)$), it holds that

$$c_h(\mathbf{w};\mathbf{u},\mathbf{v}):=\sum_{E\in\Omega_h}c_h^E(\mathbf{w};\mathbf{u},\mathbf{v})\leq C\sum_{E\in\Omega_h}\|\mathbf{w}\|_{L^r(E)}^{r-2}\|\mathbf{u}\|_{L^r(E)}\|\mathbf{v}\|_{L^r(E)}$$

$$
\begin{aligned}
&\leq C\Big(\sum_{E\in\Omega_h}\big(\|\mathbf{w}\|_{L^r(E)}^{r-2}\big)^{\frac{r}{r-2}}\Big)^{\frac{r-2}{r}}\Big(\sum_{E\in\Omega_h}\|\mathbf{u}\|_{L^r(E)}^{r}\Big)^{\frac{1}{r}}\Big(\sum_{E\in\Omega_h}\|\mathbf{v}\|_{L^r(E)}^{r}\Big)^{\frac{1}{r}}\\
&\leq C\|\mathbf{w}\|_{L^r(\Omega)}^{r-2}\,\|\mathbf{u}\|_{L^r(\Omega)}\,\|\mathbf{v}\|_{L^r(\Omega)}\\
&\leq C\|\mathbf{w}\|_{\mathbf{V}}^{r-2}\,\|\mathbf{u}\|_{\mathbf{V}}\,\|\mathbf{v}\|_{\mathbf{V}}.
\end{aligned}
$$

The proof is complete. □

In the following, we introduce some useful inequalities for proving the uniqueness of the divergence-free virtual element problem (3.23), and these will also be used for convergence analysis in Section 5.

Lemma 4.2 ([36]). *For any $a, b \in \mathbb{R}^d$ and $r > 2$, there holds*

$$\big||a|^{r-2} - |b|^{r-2}\big| \leq C\left(|a|^{r-3} - |b|^{r-3}\right)|a-b|, \tag{4.3a}$$

$$\big||a|^{r-2}a - |b|^{r-2}b\big| \leq C\big(|a| + |b|\big)^{r-2}|a-b|, \tag{4.3b}$$

$$\big||a|^{r-2} - |b|^{r-2} - (r-2)|b|^{r-4}b(a-b)\big| \leq C\left(|a|^{r-4} - |b|^{r-4}\right)|a-b|^2, \tag{4.3c}$$

$$\big(|a|^{r-2}a - |b|^{r-2}b, a-b\big) \geq |a-b|^r. \tag{4.3d}$$

To prove the existence of the solution for the problem (3.23), we introduce the following topological degree lemma (as outlined in [26]).

Lemma 4.3. *Let Y be a finite dimensional functional space equipped with a norm $\|\cdot\|_Y$, $\theta > 0$ and $\Psi : Y \times [0,1] \to Y$, satisfying the following assumptions:*

(i) *Ψ is continuous;*

(ii) *for any $(y,\lambda) \in Y \times [0,1]$, $\Psi(y,\lambda) = 0$ implies $\|y\|_Y \neq \theta$;*

(iii) *$\Psi(\cdot,0)$ is an affine function and the equation $\Psi(Y,0) = 0$ has a solution $y \in Y$ such that $\|y\|_Y < \theta$.*

Then, there exists $y \in Y$ such that $\Psi(y,1) = 0$ and $\|y\|_Y < \theta$.

Utilizing the lemmas presented above, we now provide the result of the well-posedness for the divergence-free virtual element problem (3.23).

Theorem 4.1 (Existence and Boundedness). *Assume $\mathbf{f}_h \in [H^{-1}(\Omega)]^2$ and $\nu \in L^\infty(\Omega)$ is a uniformly positive constant. There exists a solution $\mathbf{u}_h \in \mathbf{Z}_h$ of the discrete divergence-free virtual element problem* (3.23) *satisfying the following estimate:*

$$\|\mathbf{u}_h\|_{\mathbf{V}} \leq \frac{\|\mathbf{f}_h\|_{-1}}{\alpha_*\nu} := \gamma_h, \tag{4.4}$$

where α_*, derived from (3.13)*, is a constant independent of h but dependent on k.*

Proof. Let $Y_h := \mathbf{Z}_h$. It is obvious that Y_h is a finite dimensional functional space. For any $\mathbf{w} \in Y_h$, the norm $\|\mathbf{w}\|_{Y_h}$ is given by

$$\|\mathbf{w}\|_{Y_h} := \|\mathbf{w}\|_{\mathbf{V}}.$$

Then we define the mapping $\Psi_h : Y_h \times [0,1] \to Y_h$ such that, for $(\mathbf{w}_h, \lambda) \in Y_h \times [0,1]$, $\boldsymbol{\xi}_h = \Psi(\mathbf{w}_h, \lambda)$ is defined as the unique solution to the following equation:

$$(\boldsymbol{\xi}_h, \mathbf{v}_h)_{\mathbf{V}} = \nu\, a_h(\mathbf{w}_h, \mathbf{v}_h) + \lambda\alpha\, c_h(\mathbf{w}_h; \mathbf{w}_h, \mathbf{v}_h) - (\mathbf{f}_h, \mathbf{v}_h) \tag{4.5}$$

for any $\mathbf{v}_h \in \mathbf{V}_h$. Now we check the conditions in Lemma 4.3 in turn. Firstly, it is evident that Ψ is a continuous function from the definition (4.5).

To check the second point in Lemma 4.3, let $\boldsymbol{\xi}_h = \Psi(\mathbf{w}_h, \lambda) = (\mathbf{0}, 0)$ for some $\lambda \in [0,1]$. Taking $\mathbf{v}_h = \mathbf{w}_h$ in (4.5) and using (3.15), we have

$$\begin{aligned}
&\nu \|\mathbf{w}_h\|_{\mathbf{V}}^2 = \nu a(\mathbf{w}_h, \mathbf{w}_h) \\
\le\ & \frac{\nu}{\alpha_*} a_h(\mathbf{w}_h, \mathbf{w}_h) \\
\le\ & \frac{1}{\alpha_*}\left(\nu\, a_h(\mathbf{w}_h, \mathbf{w}_h) + \lambda\alpha \sum_{E\in\Omega_h} \left\|\Pi_k^{0,E}\mathbf{w}_h\right\|_{L^r(E)}^r\right) \\
=\ & \frac{1}{\alpha_*}\big(\nu\, a_h(\mathbf{w}_h, \mathbf{w}_h) + \lambda\alpha c_h(\mathbf{w}_h; \mathbf{w}_h, \mathbf{w}_h)\big) \\
=\ & \frac{1}{\alpha_*}(\mathbf{f}_h, \mathbf{w}_h),
\end{aligned}$$

then

$$\|\mathbf{w}_h\|_{\mathbf{V}} \le \frac{(\mathbf{f}_h, \mathbf{w}_h)}{\alpha_*\nu\|\mathbf{w}_h\|_{\mathbf{V}}} \le \frac{\|\mathbf{f}_h\|_{-1}}{\alpha_*\nu}. \tag{4.6}$$

Taking into account the inequality (4.6), we consider that

$$\theta = \frac{\|\mathbf{f}_h\|_{-1}}{\alpha_*\nu} + \delta,$$

where δ is a positive constant. It is obviously that $\|\mathbf{w}_h\| \neq \theta$, then the second point in Lemma 4.3 is verified.

Finally, we check the third point in Lemma 4.3. Note that $\Psi(\mathbf{z}_h, 0)$ is an affine mapping when $\lambda = 0$. The equation $\Psi(\mathbf{z}_h, 0) = \mathbf{0}$ is equivalent to the divergence-free virtual element scheme of the Stokes equations without damping, i.e.: Find $\mathbf{z}_h \in \mathbf{Z}_h$ such that

$$\nu\, a_h(\mathbf{z}_h, \mathbf{v}_h) = (\mathbf{f}_h, \mathbf{v}_h) \quad \text{for all} \quad \mathbf{v}_h \in \mathbf{Z}_h$$

as noticed in [24], whose well-posedness is easy to prove, due to the evident stability (see (3.11), (3.13) and (3.15)) of the discrete bilinear form $a_h(\cdot,\cdot)$ with respect to the norm of $\mathbf{V}$. Denote the solution by $\mathbf{z}_h = \mathbf{w}_h \in Y_h$. Then the solution satisfies the estimate $\|\mathbf{w}_h\|_{Y_h} < \theta$. According to Lemma 4.3, there exists $\mathbf{z}_h^* = \mathbf{u}_h \in Y_h$ such that

$\Psi\left(\mathbf{z}_h^*, 1\right) = 0$ and $\|\mathbf{z}_h^*\|_{Y_h} < \theta$. From the definition of Ψ, we know that $\mathbf{u}_h$ is a solution of divergence-free virtual element problem (3.23), and satisfies (4.4). The proof is complete. □

Finally, we prove the uniqueness of the virtual element solution $\mathbf{u}_h$.

Theorem 4.2 (Uniqueness)**.** *The solution of the divergence-free virtual element problem* (3.23) *is unique.*

Proof. Let $\mathbf{u}_{h1}, \mathbf{u}_{h2} \in \mathbf{Z}_h$ be two solutions of the problem (3.23) satisfying the priori bound (4.4). Then we have, for any $\mathbf{v}_h \in \mathbf{Z}_h$

$$\begin{aligned}&\nu\, a_h\left(\mathbf{u}_{h1} - \mathbf{u}_{h2}, \mathbf{v}_h\right)\\ &\quad + \alpha \sum_{E\in\Omega_h} \left(\left|\Pi_k^{0,E}\mathbf{u}_{h1}\right|^{r-2}\Pi_k^{0,E}\mathbf{u}_{h1} - \left|\Pi_k^{0,E}\mathbf{u}_{h2}\right|^{r-2}\Pi_k^{0,E}\mathbf{u}_{h2}, \Pi_k^{0,E}\mathbf{v}_h\right)_E = 0. \qquad (4.7)\end{aligned}$$

Taking $\mathbf{v}_h = \mathbf{u}_{h1} - \mathbf{u}_{h2}$ in (4.7), we have

$$\begin{aligned}&\nu\, a_h\left(\mathbf{u}_{h1} - \mathbf{u}_{h2}, \mathbf{u}_{h1} - \mathbf{u}_{h2}\right)\\ &\quad + \alpha \sum_{E\in\Omega_h} \left(\left|\Pi_k^{0,E}\mathbf{u}_{h1}\right|^{r-2}\Pi_k^{0,E}\mathbf{u}_{h1} - \left|\Pi_k^{0,E}\mathbf{u}_{h2}\right|^{r-2}\Pi_k^{0,E}\mathbf{u}_{h2}, \Pi_k^{0,E}\mathbf{u}_{h1} - \Pi_k^{0,E}\mathbf{u}_{h2}\right)_E = 0.\end{aligned}$$

From inequality (4.3d) in Lemma 4.2 and (3.15), we know that

$$\nu\alpha_*\, \|\mathbf{u}_{h1} - \mathbf{u}_{h2}\|_{\mathbf{V}}^2 + \alpha \sum_{E\in\Omega_h} \left\|\Pi_k^{0,E}\mathbf{u}_{h1} - \Pi_k^{0,E}\mathbf{u}_{h2}\right\|_{L^r(E)}^r \le 0,$$

which means $\mathbf{u}_{h1} = \mathbf{u}_{h2}$. The proof is complete. □

5. Error analysis

The goal of this section is to derive optimal error estimates for the velocity and pressure. To accomplish this, we will first introduce an interpolation error estimate and four technical lemmas. Subsequently, the optimal error estimates will be derived.

5.1. Interpolation estimate

In this subsection, we provide the following classical interpolation estimate for the enhanced space $\mathbf{V}_h$, as detailed in [25, 42].

Theorem 5.1. *Let $\mathbf{v} \in H^{s+1}(\Omega) \cap \mathbf{V}$ for $0 \le s \le k$. Then there exists an approximation $\mathbf{v}_I \in \mathbf{V}_h$ such that*

$$\|\mathbf{v} - \mathbf{v}_I\|_0 + h\|\mathbf{v} - \mathbf{v}_I\|_{\mathbf{V}} \le Ch^{s+1}|\mathbf{v}|_{s+1}, \qquad (5.1)$$

where the constant C is only dependent on the degree k and the shape regularity constant ρ (see Assumption 3.1*).*

5.2. Convergence analysis

To establish the optimal error estimate, we need to introduce the following lemmas. First, we present the following classical approximation result for the $\mathbb{P}_k$ space on star-shaped domains [5].

Lemma 5.1. *Let $E \in \Omega_h$, and let two real numbers s, p with $0 \le s \le k$ and $1 \le p \le \infty$. Then for all $\mathbf{u} \in [H^{s+1}(\Omega)]^2$, there exists a polynomial function $\mathbf{u}_\pi \in [\mathbb{P}_k(\Omega)]^2$ such that*

$$\|\mathbf{u} - \mathbf{u}_\pi\|_{L^p(E)} + h_E|\mathbf{u} - \mathbf{u}_\pi|_{W^{1,p}(E)} \le Ch_E^{s+1}|\mathbf{u}|_{W^{s+1,p}(E)} \tag{5.2}$$

with C only depending on k and the shape regularity constant ρ in Assumption 3.1.

Lemma 5.2. *Let $\mathbf{v} \in H^{s+1}(\Omega) \cap \mathbf{V}$ with $0 \le s \le k$. Then for all $\mathbf{w} \in \mathbf{V}$, it holds that*

$$|c(\mathbf{v}; \mathbf{v}, \mathbf{w}) - c_h(\mathbf{v}; \mathbf{v}, \mathbf{w})| \le Ch^s(\|\mathbf{v}\|_{s+1} + \|\mathbf{v}\|_s)\|\mathbf{v}\|_{\mathbf{V}}^{r-2}\|\mathbf{w}\|_{\mathbf{V}}.$$

Proof. First, by definition (2.4) and (3.12), we obtain that

$$\begin{aligned}
&c(\mathbf{v}; \mathbf{v}, \mathbf{w}) - c_h(\mathbf{v}; \mathbf{v}, \mathbf{w}) \\
:=& \sum_{E\in\Omega_h} \int_E |\mathbf{v}|^{r-2}\mathbf{v}\cdot\mathbf{w} - \left|\Pi_k^{0,E}\mathbf{v}\right|^{r-2}\Pi_k^{0,E}\mathbf{v}\cdot\Pi_k^{0,E}\mathbf{w}\,\mathrm{d}\mathbf{x} \\
=& \sum_{E\in\Omega_h} \int_E \left(|\mathbf{v}|^{r-2}\mathbf{v}\cdot\mathbf{w} - |\mathbf{v}|^{r-2}\mathbf{v}\cdot\Pi_k^{0,E}\mathbf{w}\right) \\
&\quad + \left(|\mathbf{v}|^{r-2}\mathbf{v}\cdot\Pi_k^{0,E}\mathbf{w} - \left|\Pi_k^{0,E}\mathbf{v}\right|^{r-2}\Pi_k^{0,E}\mathbf{v}\cdot\Pi_k^{0,E}\mathbf{w}\right)\,\mathrm{d}\mathbf{x} \\
:=& \sum_{E\in\Omega_h} \int_E \mathcal{A}(\mathbf{w}) + \mathcal{B}(\mathbf{w})\,\mathrm{d}\mathbf{x}.
\end{aligned}$$

Then, we estimate the right hand side of (5.2) term by term. For the term $\int_E \mathcal{A}(\mathbf{w})\,\mathrm{d}\mathbf{x}$, by definition of L^2 projection $\Pi_k^{0,E}$, Hölder inequality, the continuity of $\Pi_k^{0,E}$ with respect to L^6-norm (see Lemma 4.1) and Lemma 5.1, we have

$$\begin{aligned}
\int_E \mathcal{A}(\mathbf{w})\,\mathrm{d}\mathbf{x} :=& \int_E |\mathbf{v}|^{r-2}\mathbf{v}\left(\mathbf{w} - \Pi_k^{0,E}\mathbf{w}\right)\,\mathrm{d}\mathbf{x} \\
=& \int_E \left[(I - \Pi_{k-2}^{0,E})|\mathbf{v}|^{r-2}\mathbf{v}\right]\left(\mathbf{w} - \Pi_k^{0,E}\mathbf{w}\right)\,\mathrm{d}\mathbf{x} \\
\le& \left\|(I - \Pi_{k-2}^{0,E})|\mathbf{v}|^{r-2}\right\|_{L^6(E)}\left\|(I - \Pi_{k-2}^{0,E})\mathbf{v}\right\|_{L^3(E)}\left\|(I - \Pi_k^{0,E})\mathbf{w}\right\|_{0,E} \\
\le& C\left(\left\||\mathbf{v}|^{r-2}\right\|_{L^6(E)} + \left\|\Pi_{k-2}^{0,E}|\mathbf{v}|^{r-2}\right\|_{L^6(E)}\right)\left\|(I - \Pi_k^{0,E})\mathbf{v}\right\|_{L^3(E)} h_E|\mathbf{w}|_{1,E} \\
\le& Ch_E\left\||\mathbf{v}|^{r-2}\right\|_{L^6(E)}\left\|(I - \Pi_{k-2}^{0,E})\mathbf{v}\right\|_{L^3(E)}|\mathbf{w}|_{1,E} \\
\le& Ch_E^s\left\||\mathbf{v}|^{r-2}\right\|_{L^6(E)}\|\mathbf{v}\|_{W^{s-1,3}(E)}|\mathbf{w}|_{1,E}.
\end{aligned}$$

Applying once again the Hölder inequality (for sequences), we get

$$\begin{aligned}
&\sum_{E\in\Omega_h}\int_E \mathcal{A}(\mathbf{w})\,\mathrm{d}\mathbf{x}\\
&\le Ch^s\sum_{E\in\Omega_h}\big\||\mathbf{v}|^{r-2}\big\|_{L^6(E)}\|\mathbf{v}\|_{W^{s-1,3}(E)}|\mathbf{w}|_{1,E}\\
&\le Ch^s\bigg(\sum_{E\in\Omega_h}\big\||\mathbf{v}|^{r-2}\big\|^6_{L^6(E)}\bigg)^{\frac{1}{6}}\bigg(\sum_{E\in\Omega_h}\|\mathbf{v}\|^3_{W^{s-1,3}(E)}\bigg)^{\frac{1}{3}}\bigg(\sum_{E\in\Omega_h}|\mathbf{w}|^2_{1,E}\bigg)^{\frac{1}{2}}\\
&= Ch^s\big\||\mathbf{v}|^{r-2}\big\|_{L^6(\Omega)}\|\mathbf{v}\|_{W^{s-1,3}(\Omega)}\|\mathbf{w}\|_{\mathbf{V}}\\
&= Ch^s\|\mathbf{v}\|^{r-2}_{L^{6r-12}(\Omega)}\|\mathbf{v}\|_{W^{s-1,3}(\Omega)}\|\mathbf{w}\|_{\mathbf{V}}.
\end{aligned}$$

Then by the Sobolev embedding theorem, i.e. $H^1(\Omega)\hookrightarrow L^{6r-12}(\Omega)$ and $H^s(\omega)\hookrightarrow W^{s-1,4}(\Omega)$, we obtain

$$\sum_{E\in\Omega_h}\int_E \mathcal{A}(\mathbf{w})\,\mathrm{d}\mathbf{x}\le\ Ch^s\|\mathbf{v}\|^{r-2}_{\mathbf{V}}\|\mathbf{v}\|_s\|\mathbf{w}\|_{\mathbf{V}}. \tag{5.3}$$

For the second term $\int_E\mathcal{B}(\mathbf{w})\,\mathrm{d}\mathbf{x}$, by using (4.3b), Hölder inequality, the continuity of $\Pi^{0,E}_k$ with respect to L^{4r-8}-norm and L^4-norm, embedding theorem and Lemma 5.1, we obtain

$$\begin{aligned}
\int_E\mathcal{B}(\mathbf{w})\,\mathrm{d}\mathbf{x}&=\int_E\Big(|\mathbf{v}|^{r-2}\mathbf{v}-\big|\Pi^{0,E}_k\mathbf{v}\big|^{r-2}\Pi^{0,E}_k\mathbf{v}\Big)\,\Pi^{0,E}_k\mathbf{w}\,\mathrm{d}\mathbf{x}\\
&\le C\int_E\big|\mathbf{v}-\Pi^{0,E}_k\mathbf{v}\big|\Big(|\mathbf{v}|+\big|\Pi^{0,E}_k\mathbf{v}\big|\Big)^{r-2}\big|\Pi^{0,E}_k\mathbf{w}\big|\,\mathrm{d}\mathbf{x}\\
&\le C\int_E\big|\mathbf{v}-\Pi^{0,E}_k\mathbf{v}\big|\Big(|\mathbf{v}|^{r-2}+\big|\Pi^{0,E}_k\mathbf{v}\big|^{r-2}\Big)\big|\Pi^{0,E}_k\mathbf{w}\big|\,\mathrm{d}\mathbf{x}\\
&\le C\big\|\mathbf{v}-\Pi^{0,E}_k\mathbf{v}\big\|_{0,E}\Big(\big\||\mathbf{v}|^{r-2}\big\|_{L^4(E)}+\big\|\big|\Pi^{0,E}_k\mathbf{v}\big|^{r-2}\big\|_{L^4(E)}\Big)\big\|\Pi^{0,E}_k\mathbf{w}\big\|_{L^4(E)}\\
&\le C|\mathbf{v}-\Pi^{0,E}_k\mathbf{v}|_{1,E}\Big(\|\mathbf{v}\|^{r-2}_{L^{4r-8}(E)}+\big\|\Pi^{0,E}_k\mathbf{v}\big\|^{r-2}_{L^{4r-8}(E)}\Big)\|\mathbf{w}\|_{L^4(E)}\\
&\le Ch^s_E|\mathbf{v}|_{s+1,E}\|\mathbf{v}\|^{r-2}_{L^{4r-8}(E)}\|\mathbf{w}\|_{L^4(E)}\\
&= Ch^s_E|\mathbf{v}|_{s+1,E}\cdot\big\||\mathbf{v}|^{r-2}\big\|_{L^4(E)}\|\mathbf{w}\|_{L^4(E)}.
\end{aligned}$$

Applying the Hölder inequality, we have

$$\begin{aligned}
&\sum_{E\in\Omega_h}\int_E\mathcal{B}(\mathbf{w})\,\mathrm{d}\mathbf{x}\\
&\le Ch^s\sum_{E\in\Omega_h}|\mathbf{v}|_{s+1,E}\big\||\mathbf{v}|^{r-2}\big\|_{L^4(E)}\|\mathbf{w}\|_{L^4(E)}\\
&\le Ch^s\bigg(\sum_{E\in\Omega_h}|\mathbf{v}|^2_{s+1,E}\bigg)^{\frac{1}{2}}\bigg(\sum_{E\in\Omega_h}\big\||\mathbf{v}|^{r-2}\big\|^4_{L^4(E)}\bigg)^{\frac{1}{4}}\bigg(\sum_{E\in\Omega_h}\|\mathbf{w}\|^4_{L^4(E)}\bigg)^{\frac{1}{4}}
\end{aligned}$$

$$= Ch^s|\mathbf{v}|_{s+1}\left\||\mathbf{v}|^{r-2}\right\|_{L^4(\Omega)}\|\mathbf{w}\|_{L^4(\Omega)}$$
$$= Ch^s|\mathbf{v}|_{s+1}\|\mathbf{v}\|^{r-2}_{L^{4r-8}(\Omega)}\|\mathbf{w}\|_{L^4(\Omega)}.$$

And by using the Sobolev embedding theorem, i.e. $H^1(\Omega) \hookrightarrow L^{4r-8}(\Omega)$ and $H^1(\Omega) \hookrightarrow L^4(\Omega)$, we obtain

$$\sum_{E\in\Omega_h}\int_E \mathcal{B}(\mathbf{w})\,\mathrm{d}\mathbf{x} \le Ch^s\|\mathbf{v}\|_{s+1}\|\mathbf{v}\|^{r-2}_{\mathbf{V}}\|\mathbf{w}\|_{\mathbf{V}}. \tag{5.4}$$

By combining (5.3) and (5.4) in (5.2), we conclude that

$$|c(\mathbf{v};\mathbf{v},\mathbf{w}) - c_h(\mathbf{v};\mathbf{v},\mathbf{w})| \le Ch^s(\|\mathbf{v}\|_{s+1} + \|\mathbf{v}\|_s)\|\mathbf{v}\|^{r-2}_{\mathbf{V}}\|\mathbf{w}\|_{\mathbf{V}}, \tag{5.5}$$

and the proof is complete. □

Lemma 5.3. *For any* $\mathbf{v},\mathbf{z},\mathbf{w}\in\mathbf{V}$*, it holds that*

$$|c_h(\mathbf{v};\mathbf{v},\mathbf{w}) - c_h(\mathbf{z};\mathbf{z},\mathbf{w})| \le C\left(\|\mathbf{v}\|^{r-2}_{\mathbf{V}} + \|\mathbf{z}\|^{r-2}_{\mathbf{V}}\right)\|\mathbf{v}-\mathbf{z}\|_{\mathbf{V}}\,\|\mathbf{w}\|_{\mathbf{V}}.$$

Proof. By the definition (3.12) and inequality (4.3b) in Lemma 4.2, we have

$$\begin{aligned}
&|c_h(\mathbf{v};\mathbf{v},\mathbf{w}) - c_h(\mathbf{z};\mathbf{z},\mathbf{w})|\\
&= \left|\sum_{E\in\Omega_h}\int_E \left(\left|\Pi_k^{0,E}\mathbf{v}\right|^{r-2}\Pi_k^{0,E}\mathbf{v} - \left|\Pi_k^{0,E}\mathbf{z}\right|^{r-2}\Pi_k^{0,E}\mathbf{z}\right)\Pi_k^{0,E}\mathbf{w}\,\mathrm{d}\mathbf{x}\right|\\
&\le \sum_{E\in\Omega_h}\int_E \left(\left|\Pi_k^{0,E}\mathbf{v}\right| + \left|\Pi_k^{0,E}\mathbf{z}\right|\right)^{r-2}\left|\Pi_k^{0,E}\mathbf{v} - \Pi_k^{0,E}\mathbf{z}\right|\left|\Pi_k^{0,E}\mathbf{w}\right|\,\mathrm{d}\mathbf{x}\\
&\le \sum_{E\in\Omega_h}\int_E \left(\left|\Pi_k^{0,E}\mathbf{v}\right|^{r-2} + \left|\Pi_k^{0,E}\mathbf{z}\right|^{r-2}\right)\left|\Pi_k^{0,E}\mathbf{v} - \Pi_k^{0,E}\mathbf{z}\right|\left|\Pi_k^{0,E}\mathbf{w}\right|\,\mathrm{d}\mathbf{x}\\
&= \sum_{E\in\Omega_h}\left[\int_E \left|\Pi_k^{0,E}\mathbf{v}\right|^{r-2}\left|\Pi_k^{0,E}\mathbf{v} - \Pi_k^{0,E}\mathbf{z}\right|\left|\Pi_k^{0,E}\mathbf{w}\right|\,\mathrm{d}\mathbf{x}\right.\\
&\qquad\qquad \left. + \int_E \left|\Pi_k^{0,E}\mathbf{z}\right|^{r-2}\left|\Pi_k^{0,E}\mathbf{v} - \Pi_k^{0,E}\mathbf{z}\right|\left|\Pi_k^{0,E}\mathbf{w}\right|\,\mathrm{d}\mathbf{x}\right]\\
&=: \sum_{E\in\Omega_h}\int_E \mu_1(\mathbf{w}) + \mu_2(\mathbf{w})\,\mathrm{d}\mathbf{x}.
\end{aligned}\tag{5.6}$$

By using the Hölder inequality, the continuity (4.2) of $\Pi_k^{0,E}$, and Sobolev embedding theorem ($H^1(\Omega)\hookrightarrow L^r(\Omega)$), the term $\sum_{E\in\Omega_h}\int_E \mu_1(\mathbf{w})\,\mathrm{d}\mathbf{x}$ can be estimated as

$$\begin{aligned}
&\sum_{E\in\Omega_h}\int_E \mu_1(\mathbf{w})\,\mathrm{d}\mathbf{x}\\
&:= \sum_{E\in\Omega_h}\int_E \left|\Pi_k^{0,E}\mathbf{v}\right|^{r-2}\left|\Pi_k^{0,E}\mathbf{v} - \Pi_k^{0,E}\mathbf{z}\right|\left|\Pi_k^{0,E}\mathbf{w}\right|\,\mathrm{d}\mathbf{x}
\end{aligned}$$

$$
\begin{aligned}
&\leq \sum_{E\in\Omega_h} \left\|\Pi_k^{0,E}\mathbf{v}\right\|_{L^r(E)}^{r-2}\left\|\Pi_k^{0,E}\mathbf{w}\right\|_{L^r(E)}\left\|\Pi_k^{0,E}(\mathbf{v}-\mathbf{z})\right\|_{L^r(E)}\\
&\leq C\sum_{E\in\Omega_h} \|\mathbf{v}\|_{L^r(E)}^{r-2}\|\mathbf{w}\|_{L^r(E)}\cdot\|\mathbf{v}-\mathbf{z}\|_{L^r(E)}\\
&\leq C\Bigg(\sum_{E\in\Omega_h}\Big(\|\mathbf{v}\|_{L^r(E)}^{r-2}\Big)^{\frac{r}{(r-2)}}\Bigg)^{\frac{(r-2)}{r}}\Bigg(\sum_{E\in\Omega_h}\|\mathbf{w}\|_{L^r(E)}^{r}\Bigg)^{\frac{1}{r}}\Bigg(\sum_{E\in\Omega_h}\|\mathbf{v}-\mathbf{z}\|_{L^r(E)}^{r}\Bigg)^{\frac{1}{r}}\\
&\leq C\|\mathbf{v}\|_{L^r(\Omega)}^{r-2}\|\mathbf{w}\|_{L^r(\Omega)}\|\mathbf{v}-\mathbf{z}\|_{L^r(\Omega)}\\
&\leq C\|\mathbf{v}\|_{\mathbf{V}}^{r-2}\|\mathbf{w}\|_{\mathbf{V}}\|\mathbf{v}-\mathbf{z}\|_{\mathbf{V}}. \qquad (5.7)
\end{aligned}
$$

Following same arguments as (5.7), we obtain that

$$\sum_{E\in\Omega_h}\int_E \mu_2(\mathbf{w})\,\mathrm{d}\mathbf{x} \leq C\|\mathbf{z}\|_{\mathbf{V}}^{r-2}\|\mathbf{w}\|_{\mathbf{V}}\|\mathbf{v}-\mathbf{z}\|_{\mathbf{V}}. \qquad (5.8)$$

We infer the proof by combining (5.7) and (5.8) in (5.6). □

Furthermore, we state the following result concerning the load approximation, which can be proved using the standard arguments [17].

Lemma 5.4. *Let $\mathbf{f}_h$ be defined as in* (3.18)*, and assume $\mathbf{f}\in H^{s+1}(\Omega)$, $-1\leq s\leq k$. Then for all $\mathbf{v}_h\in\mathbf{V}_h$, it holds that*

$$|(\mathbf{f}_h-\mathbf{f},\mathbf{v}_h)| \leq Ch^{s+2}\,|\mathbf{f}|_{s+1}\,\|\mathbf{v}_h\|_{\mathbf{V}}\,.$$

We observe that for a given $\mathbf{v}\in\mathbf{Z}$, the application of the inf-sup condition (3.22) (see [4] for detail) leads to the following inequality:

$$\inf_{\mathbf{v}_h\in\mathbf{Z}_h,\mathbf{v}_h\neq\mathbf{0}}\|\mathbf{v}-\mathbf{v}_h\|_{\mathbf{V}} \leq C\inf_{\mathbf{w}_h\in\mathbf{V}_h,\mathbf{w}_h\neq\mathbf{0}}\|\mathbf{v}-\mathbf{w}_h\|_{\mathbf{V}},$$

which implies that the $\mathbf{Z}$ can be approximated by subspace $\mathbf{Z}_h$ with an accuracy order equivalent to that of the entire space $\mathbf{V}_h$. In particular, applying Theorem 5.1 and assuming $\mathbf{v}\in H^{s+1}(\Omega)\cap\mathbf{Z}$, $0<s\leq k$, we can obtain

$$\inf_{\mathbf{v}_h\in\mathbf{Z}_h,\mathbf{v}_h\neq\mathbf{0}}\|\mathbf{v}-\mathbf{v}_h\|_{\mathbf{V}} \leq Ch^{s}\,|\mathbf{v}|_{s+1}\,. \qquad (5.9)$$

Subsequently, we establish optimal error estimates for the velocity and pressure.

Theorem 5.2. *Under Assumption* 3.1*, let $\mathbf{u}$ and $\mathbf{u}_h$ be solutions of the divergence-free problem* (2.10) *and divergence-free virtual element problem* (3.23)*, respectively. Setting $\mathbf{u},\mathbf{f}\in[H^{s+1}(\Omega)]^2$ for $0<s\leq k$, we have*

$$\|\mathbf{u}-\mathbf{u}_h\|_{\mathbf{V}} \leq h^s\mathcal{F}(\mathbf{u};\nu,\alpha_*,\gamma)+Ch^{s+2}|\mathbf{f}|_{s+1}, \qquad (5.10)$$

where $\mathcal{F}$ is a suitable function independent of h.

Proof. Subtracting (2.10) from (3.23), we have the following error equation, for any $(\mathbf{v}_h, q_h) \in \mathbf{V}_h \times Q_h$:

$$\begin{aligned} &\nu a(\mathbf{u}, \mathbf{v}_h) - \nu a_h(\mathbf{u}_h, \mathbf{v}_h) + \alpha c(\mathbf{u}; \mathbf{u}, \mathbf{v}_h) \\ &\quad - \alpha c_h(\mathbf{u}_h; \mathbf{u}_h, \mathbf{v}_h) - (\mathbf{f}, \mathbf{v}_h) + (\mathbf{f}_h, \mathbf{v}_h) = 0. \end{aligned} \tag{5.11}$$

Let $\mathbf{w}_h$ be an approximant of $\mathbf{u}$ in the discrete divergence-free space $\mathbf{Z}_h$ satisfying (5.9). And setting $\mathbf{e}_h = \mathbf{u}_h - \mathbf{w}_h$, it holds that $\mathbf{e}_h \in \mathbf{Z}_h$. Then, selecting $\mathbf{v}_h = \mathbf{e}_h$ in the error equation (5.11), we get

$$\begin{aligned} &\nu a_h(\mathbf{e}_h, \mathbf{e}_h) + \alpha c_h(\mathbf{u}_h; \mathbf{u}_h, \mathbf{e}_h) - \alpha c_h(\mathbf{w}_h; \mathbf{w}_h, \mathbf{e}_h) \\ &= \big\{\nu a(\mathbf{u}, \mathbf{e}_h) - \nu a_h(\mathbf{w}_h, \mathbf{e}_h)\big\} + \big\{\alpha c(\mathbf{u}; \mathbf{u}, \mathbf{e}_h) - \alpha c_h(\mathbf{w}_h; \mathbf{w}_h, \mathbf{e}_h)\big\} + (\mathbf{f}_h - \mathbf{f}, \mathbf{e}_h). \end{aligned} \tag{5.12}$$

From the inequality (4.3d) in Lemma 4.2 and using the definition (3.12) of trilinear form $c_h(\cdot;\cdot,\cdot)$, we have

$$\begin{aligned} &c_h(\mathbf{u}_h; \mathbf{u}_h, \mathbf{e}_h) - c_h(\mathbf{w}_h; \mathbf{w}_h, \mathbf{e}_h) \\ &= \Big(\big|\Pi_k^{0,E}\mathbf{u}_h\big|^{r-2}\Pi_k^{0,E}\mathbf{u}_h, \Pi_k^{0,E}\mathbf{e}_h\Big) - \Big(\big|\Pi_k^{0,E}\mathbf{w}_h\big|^{r-2}\Pi_k^{0,E}\mathbf{w}_h, \Pi_k^{0,E}\mathbf{e}_h\Big) \\ &= \Big(\big|\Pi_k^{0,E}\mathbf{u}_h\big|^{r-2}\Pi_k^{0,E}\mathbf{u}_h - \big|\Pi_k^{0,E}\mathbf{w}_h\big|^{r-2}\Pi_k^{0,E}\mathbf{w}_h, \Pi_k^{0,E}\mathbf{e}_h\Big) \\ &\geq \big|\Pi_k^{0,E}\mathbf{e}_h\big|^r \geq 0. \end{aligned} \tag{5.13}$$

Noting that $\alpha_*\|\mathbf{e}_h\|_{\mathbf{V}}^2 \leq a_h(\mathbf{e}_h, \mathbf{e}_h)$ and $\alpha > 0$, as well as employing the above result, we further obtain that

$$\alpha_*\nu\|\mathbf{e}_h\|_{\mathbf{V}}^2 \leq \nu a_h(\mathbf{e}_h, \mathbf{e}_h) + \alpha c_h(\mathbf{u}_h; \mathbf{u}_h, \mathbf{e}_h) - \alpha c_h(\mathbf{w}_h; \mathbf{w}_h, \mathbf{e}_h). \tag{5.14}$$

Hence, error equation (5.11) can be reduced as

$$\begin{aligned} \alpha_*\nu\|\mathbf{e}_h\|_{\mathbf{V}}^2 &\leq \big\{\nu a(\mathbf{u}, \mathbf{e}_h) - \nu a_h(\mathbf{w}_h, \mathbf{e}_h)\big\} \\ &\quad + \big\{\alpha c(\mathbf{u}; \mathbf{u}, \mathbf{e}_h) - \alpha c_h(\mathbf{w}_h; \mathbf{w}_h, \mathbf{e}_h)\big\} + (\mathbf{f}_h - \mathbf{f}, \mathbf{e}_h) \\ &=: R_1 + R_2 + R_3. \end{aligned} \tag{5.15}$$

Next, we estimate the right hand side of (5.15) term by term.

1. By using the stability (3.15) and the consistency (3.14) properties of the bilinear form $a_h(\cdot,\cdot)$, the triangular inequality, Lemma 5.1 and (5.9), we get

$$\begin{aligned} R_1 &:= \nu a(\mathbf{u}, \mathbf{e}_h) - \nu a_h(\mathbf{w}_h, \mathbf{e}_h) \\ &= \nu \sum_{E\in\Omega_h} \big(a^E(\mathbf{u} - \mathbf{u}_\pi, \mathbf{e}_h) + a_h^E(\mathbf{u}_\pi - \mathbf{w}_h, \mathbf{e}_h)\big) \\ &\leq C\nu\big(\|\mathbf{u} - \mathbf{u}_\pi\|_{\mathbf{V}}\|\mathbf{e}_h\|_{\mathbf{V}} + \|\mathbf{u} - \mathbf{w}_h\|_{\mathbf{V}}\|\mathbf{e}_h\|_{\mathbf{V}}\big) \\ &\leq Ch^s\nu|\mathbf{u}|_{s+1}\|\mathbf{e}_h\|_{\mathbf{V}} + C\nu\|\mathbf{u} - \mathbf{w}_h\|_{\mathbf{V}}\|\mathbf{e}_h\|_{\mathbf{V}} \\ &\leq Ch^s\nu|\mathbf{u}|_{s+1}\|\mathbf{e}_h\|_{\mathbf{V}}, \end{aligned} \tag{5.16}$$

where $\mathbf{u}_\pi$ is the piecewise polynomial of degree k for $\mathbf{u}$.

2. For the term R_2, using the Lemmas 5.2-5.3 and (5.9), it holds that

$$\begin{aligned}
R_2 &:= \alpha c(\mathbf{u};\mathbf{u},\mathbf{e}_h) - \alpha c_h(\mathbf{w}_h;\mathbf{w}_h,\mathbf{e}_h)\\
&= \alpha\left[c(\mathbf{u};\mathbf{u},\mathbf{e}_h) - c_h(\mathbf{u};\mathbf{u},\mathbf{e}_h)\right] + \alpha\left[c_h(\mathbf{u};\mathbf{u},\mathbf{e}_h) - c_h(\mathbf{w}_h;\mathbf{w}_h,\mathbf{e}_h)\right]\\
&\le Ch^s\left(\|\mathbf{u}\|_{s+1} + \|\mathbf{u}\|_s\right)\|\mathbf{u}\|_{\mathbf{V}}^{r-2}\|\mathbf{e}_h\|_{\mathbf{V}}\\
&\quad + C\left(\|\mathbf{u}\|_{\mathbf{V}}^{r-2} + \|\mathbf{w}_h\|_{\mathbf{V}}^{r-2}\right)\|\mathbf{u}-\mathbf{w}_h\|_{\mathbf{V}}\|\mathbf{e}_h\|_{\mathbf{V}}\\
&\le Ch^s\left[\left(\|\mathbf{u}\|_{s+1} + \|\mathbf{u}\|_s\right)\|\mathbf{u}\|_{\mathbf{V}}^{r-2} + \|\mathbf{w}_h\|^{r-2}|\mathbf{u}|_{s+1}\right]\|\mathbf{e}_h\|_{\mathbf{V}}.
\end{aligned}$$

Noting that the assumption (2.8)

$$\|\mathbf{u}\|_{\mathbf{V}} \le \frac{\|\mathbf{f}\|_{-1}}{\nu} := \gamma \le C,$$

and by applying the triangle inequality and (5.9), we have

$$\|\mathbf{w}_h\|_{\mathbf{V}} \le \|\mathbf{w}_h - \mathbf{u}\|_{\mathbf{V}} + \|\mathbf{u}\|_{\mathbf{V}} \le\ Ch^s|\mathbf{u}|_{s+1} + \|\mathbf{u}\|_{\mathbf{V}} \le\ C|\mathbf{u}|_{s+1} + \gamma.$$

Thus,

$$R_2 \le\ Ch^s\left[\left(\|\mathbf{u}\|_{s+1} + \|\mathbf{u}\|_s\right)\|\mathbf{u}\|_{\mathbf{V}}^{r-2} + |\mathbf{u}|_{s+1}^{r-1} + \gamma^{r-2}|\mathbf{u}|_{s+1}\right]\|\mathbf{e}_h\|_{\mathbf{V}}. \tag{5.17}$$

3. Utilizing the Lemma 5.4, the term R_3 can be estimated as

$$R_3 := (\mathbf{f}_h - \mathbf{f}, \mathbf{e}_h) \le Ch^{s+2}|\mathbf{f}|_{s+1}\|\mathbf{e}_h\|_{\mathbf{V}}. \tag{5.18}$$

Then combining (5.16)-(5.18) in (5.15) yields

$$\begin{aligned}
\alpha_*\nu\|\mathbf{e}_h\|_{\mathbf{V}} \le Ch^s\Big[&\nu|\mathbf{u}|_{s+1} + h^2|\mathbf{f}|_{s+1} + \left(\|\mathbf{u}\|_{s+1} + \|\mathbf{u}\|_s\right)\|\mathbf{u}\|_{\mathbf{V}}^{r-2}\\
&+ |\mathbf{u}|_{s+1}^{r-1} + \gamma^{r-2}|\mathbf{u}|_{s+1}\Big],
\end{aligned} \tag{5.19}$$

which further implies that

$$\|\mathbf{e}_h\|_{\mathbf{V}} \le h^s\mathcal{F}(\mathbf{u};\nu,\alpha_*,\gamma) + Ch^{s+2}|\mathbf{f}|_{s+1}, \tag{5.20}$$

where the function

$$\mathcal{F}(\mathbf{u};\nu,\alpha_*,\gamma) = \frac{C}{\alpha_*\nu}\left[\nu|\mathbf{u}|_{s+1} + \left(\|\mathbf{u}\|_{s+1} + \|\mathbf{u}\|_s\right)\|\mathbf{u}\|_{\mathbf{V}}^{r-2} + |\mathbf{u}|_{s+1}^{r-1} + \gamma^{r-2}|\mathbf{u}|_{s+1}\right].$$

Thus, by using the triangle inequality and (5.9) in (5.20), we complete the proof. □

Remark 5.1. The present method in this paper removes the pressure-dependence of the velocity approximation. However, the method exhibits a locking-phenomenon for $\nu \to 0$, as it is also observed for the classical divergence-free VEM [29, 54]. This phenomenon can be attributed to the projection operator $\Pi_k^{0,E}$ changes the divergence, and therefore destroys the L^2-orthogonality between discretely divergence-free test functions and arbitrary gradient fields. Fortunately, our method has the optimal convergence rate for any reasonable viscosity coefficient (e.g. $\nu = 10^{-2}$ or 1) and is only asymptotically pressure-robust for $h \to 0$. The numerical examples below demonstrate this lack of pressure-robustness.

The pressure estimate can be readily derived from the discrete inf-sup condition (3.22) using standard arguments, as outlined in [25].

Theorem 5.3. *Let* $(\mathbf{u}, p) \in \mathbf{V} \times Q$ *be the solution of weak problem* (2.2) *and* $(\mathbf{u}_h, p_h) \in \mathbf{V}_h \times Q_h$ *be the solution of virtual problem* (3.20). *Then it holds that*

$$\|p - p_h\|_Q \leq \ Ch^s|p|_s + Ch^{s+2}|\mathbf{f}|_{s+1} + h^s\kappa(\mathbf{u}; \nu, \gamma, \gamma_h), \tag{5.21}$$

where $\kappa(\cdot;\cdot,\cdot,\cdot)$ *is a suitable function independent of* h.

6. Numerical implementation

In this section, we conduct four sets of numerical experiments to evaluate the method's practical performance. We utilized the mVEM package [55] and customized it to facilitate the implementation of our numerical examples. All of the tests are preformed with the second-order VEM, i.e., k=2. The Picard iteration method is applied for the nonlinear term and set the error tolerance is $\epsilon = 10^{-10}$. To detail the proposed Picard iteration method, give $(\mathbf{u}_h^n, p_h^n)$, such that $(\mathbf{u}_h^{n+1}, p_h^{n+1})$ satisfies

$$\begin{aligned} &\nu\, a_h\left(\mathbf{u}_h^{n+1}, \mathbf{v}_h\right) + \alpha\, c_h\left(\mathbf{u}_h^n; \mathbf{u}_h^{n+1}, \mathbf{v}_h\right) + b\left(\mathbf{v}_h, p_h\right) = \left(\mathbf{f}_h, \mathbf{v}_h\right), \\ &b\left(\mathbf{u}_h^{n+1}, q_h\right) = 0 \end{aligned} \tag{6.1}$$

for all $(\mathbf{v}_h, q_h) \in \mathbf{V}_h \times Q_h$, where $n \geq 0$ is iteration parameter. Then, the Picard iteration algorithm can be outlined as follows:

Algorithm 6.1 Picard Iterative Algorithm.

1: Given tolerance ϵ and initialize an initial guess solution $(\mathbf{u}_h^0, p_h^0) = (\mathbf{0}, 0)$.
2: Set the iteration step $n = 0$.
3: Solve the discrete problem (6.1) with $n = 0$ to obtain $(\mathbf{u}_h^1, p_h^1)$.
4: **while** $\|\mathbf{u}_h^{n+1} - \mathbf{u}_h^n\|_\infty < \epsilon$ and $\|p_h^{n+1} - p_h^n\|_\infty < \epsilon$ **do**
5: Update the iteration step $n = n + 1$;
6: Solve the discrete problem (6.1) with n to obtain $(\mathbf{u}_h^{n+1}, p_h^{n+1})$.
7: **end while**

It needs to be emphasized that we cannot pointwise access to the numerical solution $\mathbf{u}_h$ within the element. In other words, we only possess information about the degrees of freedom of $\mathbf{u}_h$ and not its values at any point within the element. Consequently, we use $\Pi^0\mathbf{u}_h$ as a substitute for $\mathbf{u}_h$ to calculate the error. Considering the computable error quantity

$$\text{error}\left(\mathbf{u}, \boldsymbol{H}^1\right) := \left(\sum_{E\in\Omega_h} \left\|\boldsymbol{\nabla}\mathbf{u} - \boldsymbol{\Pi}_{k-1}^{0,E}(\boldsymbol{\nabla}\mathbf{u}_h)\right\|_{0,E}^2\right)^{\frac{1}{2}}.$$

For the error of pressures we simply compute

$$\text{error}\left(p, L^2\right) := \left(\sum_{E\in\Omega_h} \|p - p_h\|_{0,E}^2\right)^{\frac{1}{2}}.$$

Example 6.1. Let the domain be $\Omega = (0,1) \times (0,1)$, and take the parameters as $\nu = 1$, $r = 3, \alpha = 1$. We test six types of meshes in this example, as shown in Fig. 3, that is, uniform triangular mesh $\mathcal{T}^1$, uniform rectangular mesh $\mathcal{T}^2$, quadrilateral mesh $\mathcal{T}^3$ generated by perturbing the interior nodes of $\mathcal{T}^2$ with a parameter 0.3 (see [11] for detail), polygonal mesh $\mathcal{T}^4$ generated by the dual of the triangle mesh $\mathcal{T}^1$, distorted polygonal mesh $\mathcal{T}^5$, Voronoi polygonal mesh $\mathcal{T}^6$ generated by PolyMesher package [50]. The exact solution for the Eqs. (1.1) is chosen as follows:

$$\begin{cases} u_1(x,y) = 10x^2(x-1)^2y(y-1)(2y-1), \\ u_2(x,y) = -10x(x-1)(2x-1)y^2(y-1)^2, \\ p(x,y) = 10(2x-1)(2y-1), \end{cases} \tag{6.2}$$

where the load function $\mathbf{f}$ is suitably chosen.

We conducted tests on six different mesh types and the obtained results are presented in Tables 1-3. We listed the result of errors on two successive meshes and the

Table 1: The errors for a series of the uniform triangular meshes $\mathcal{T}^1$ (upper) and uniform rectangular meshes $\mathcal{T}^2$ (below) for Example 6.1.

mesh	# Dof	h	$\mathrm{error}(\mathbf{u}, \boldsymbol{H}^1)$	order	$\mathrm{error}(p, L^2)$	order
$\mathcal{T}^1$	226	1.768e-01	5.95238e-02	-	1.54626e-01	-
	1046	7.857e-02	1.43369e-02	1.76	3.97800e-02	1.67
	3202	4.419e-02	5.03761e-03	1.82	1.44408e-02	1.76
	7702	2.828e-02	2.18255e-03	1.87	6.33725e-03	1.85
	29206	1.443e-02	5.93595e-04	1.93	1.73744e-03	1.92
$\mathcal{T}^2$	242	2.000e-01	3.88289e-02	-	1.30865e-01	-
	882	1.000e-01	1.04228e-02	1.90	3.27082e-02	2.00
	1922	6.667e-02	4.69530e-03	1.97	1.45373e-02	2.00
	5202	4.000e-02	1.70197e-03	1.99	5.23357e-03	2.00
	10658	2.778e-02	8.22414e-04	1.99	2.52393e-03	2.00

Table 2: The errors for a series of the quadrilateral meshes $\mathcal{T}^3$ (upper) and polygonal meshes $\mathcal{T}^4$ (below) for Example 6.1.

mesh	# Dof	h	$\mathrm{error}(\mathbf{u}, \boldsymbol{H}^1)$	order	$\mathrm{error}(p, L^2)$	order
$\mathcal{T}^3$	242	2.000e-01	5.14844e-02	-	1.40774e-01	-
	882	1.000e-01	1.51945e-02	1.76	3.54895e-02	1.99
	1922	6.667e-02	6.99338e-03	1.91	1.56968e-02	2.01
	5202	4.000e-02	2.61640e-03	1.92	5.70448e-03	1.98
	10658	2.778e-02	1.30431e-03	1.91	2.76113e-03	1.99
$\mathcal{T}^4$	354	2.000e-01	7.19723e-02	-	2.31081e-01	-
	1334	1.000e-01	1.60291e-02	2.17	4.24836e-02	2.44
	3714	5.882e-02	5.08237e-03	2.16	1.29071e-02	2.25
	8502	3.846e-02	2.05324e-03	2.13	5.19902e-03	2.14
	30774	2.000e-02	5.21532e-04	2.10	1.34010e-03	2.07

Table 3: The errors for a series of the distorted polygonal meshes $\mathcal{T}^5$ (upper) and Voronoi meshes $\mathcal{T}^6$ (below) for Example 6.1.

mesh	# Dof	h	$\text{error}(\mathbf{u}, \boldsymbol{H}^1)$	order	$\text{error}(p, L^2)$	order
$\mathcal{T}^5$	354	2.000e-01	1.00805e-01	-	3.15028e-01	-
	1334	1.000e-01	3.14291e-02	1.68	8.28310e-02	1.93
	3714	5.882e-02	1.00862e-02	2.14	2.79014e-02	2.05
	8502	3.846e-02	4.03940e-03	2.15	1.16901e-02	2.05
	30774	2.000e-02	1.01548e-03	2.11	3.10411e-03	2.03
$\mathcal{T}^6$	770	1.250e-01	1.83375e-02	-	4.46046e-02	-
	1534	8.839e-02	9.19132e-03	1.99	2.15685e-02	2.10
	3074	6.250e-02	4.62813e-03	1.98	1.07248e-02	2.02
	6134	4.419e-02	2.31399e-03	2.00	5.33404e-03	2.02
	12254	3.125e-02	1.14256e-03	2.04	2.64384e-03	2.03

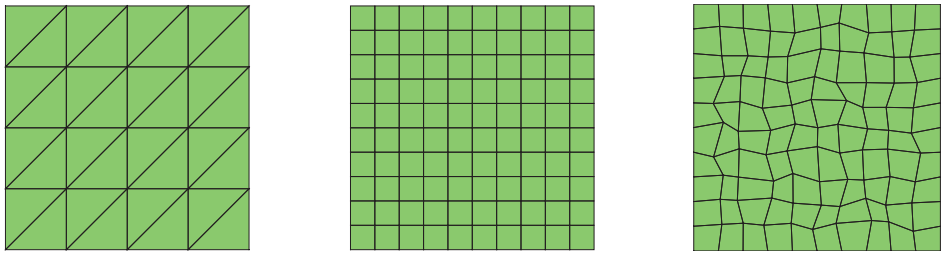

(a) $\mathcal{T}^1$ (b) $\mathcal{T}^2$ (c) $\mathcal{T}^3$

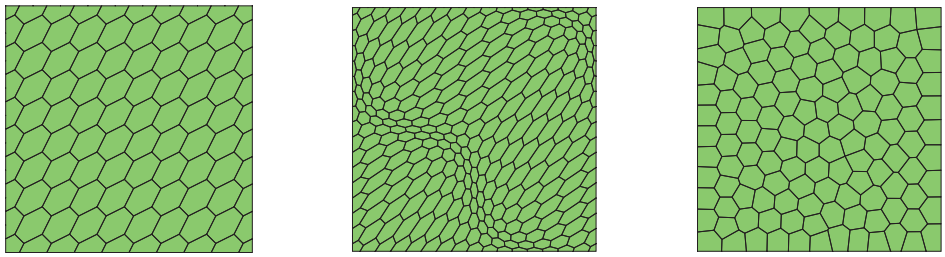

(d) $\mathcal{T}^4$ (e) $\mathcal{T}^5$ (f) $\mathcal{T}^6$

Figure 3: Illustration of meshes $\mathcal{T}^1$, $\mathcal{T}^2$, $\mathcal{T}^3$, $\mathcal{T}^4$, $\mathcal{T}^5$ and $\mathcal{T}^6$.

corresponding order of error with respect to the mesh diameter h. As expected in Theorems 5.2 and 5.3, we can observe that the errors of the numerical solution exhibit the optimal order, that is, the $\boldsymbol{H}^1$ error of the velocity and L^2 error of the pressure are of order $\mathcal{O}(h^2)$.

Example 6.2. To demonstrate the flexibility of the virtual element method (VEM) concerning mesh requirements (see Assumption 3.1 for details), we selected the parameters $\nu = 1 \times 10^{-2}$, $\alpha = 1 \times 10^{-2}$, and $r = 2.9$ for conducting numerical experiments on a series of non-convex meshes $\mathcal{T}^7$ and hybrid meshes $\mathcal{T}^8$ (as depicted in Fig. 4). Let

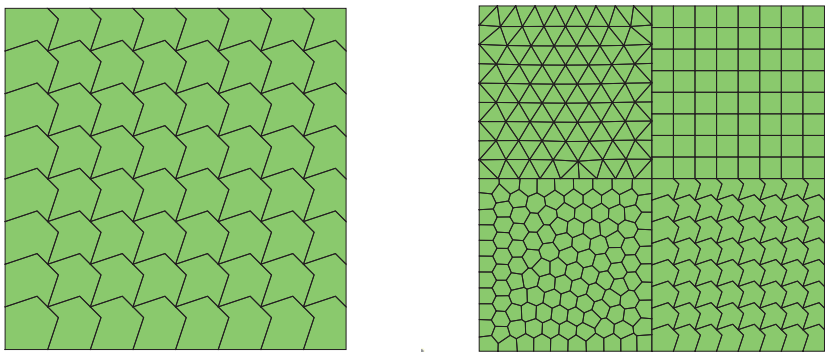

(a) non-convex mesh $\mathcal{T}^7$ (b) mixed mesh $\mathcal{T}^8$

Figure 4: Illustration of meshes $\mathcal{T}^7$ and $\mathcal{T}^8$.

$\Omega = (0,1) \times (0,1)$, and the exact solutions are given as follows:

$$\begin{cases} u_1 = -\sin(\pi x)^2 \sin(\pi y)\cos(\pi y), \\ u_2 = \sin(\pi x)\cos(\pi x)\sin(\pi y)^2, \\ p = \sin(\pi x)\cos(\pi y), \end{cases} \tag{6.3}$$

then, the source term $\mathbf{f}$ is determined by the above prescribed velocity and pressure.

In Fig. 5, we provide visual representations of both the numerical and exact solutions of velocity on a mesh with 3902 degrees of freedom. It is evident from the figures that the divergence-free virtual element method performs well for steady Stokes equations with damping. Similar to Example 6.1, we conducted numerical experiments to determine the error convergence rate between two successive non-convex meshes and mixed meshes, and the results are presented in Table 4. Notably, achieving the optimal error convergence rate even on non-convex and mixed meshes underscores the excellent flexibility of the VEM in handling complex domains.

Example 6.3. In this example, we investigate the influence of the viscosity and damping coefficients, denoted as ν and α respectively. We will choose different values for ν to verify the convergence of the problem on the Voronoi polygonal mesh $\mathcal{T}^6$, and explore the effect of damping coefficient α on the number of iterations on non-convex mesh $\mathcal{T}^7$. Let $\Omega = (0,1) \times (0,1)$, and without loss of generality, we utilize the same exact solution as presented in (6.3).

To verify the influence of the viscosity coefficient on the accuracy of the proposed method, we implement the nonlinear problem (1.1) with the viscosity coefficient $\nu = 10^{-1}, 10^{-2}, 10^{-3}, 10^{-4}, 10^{-5}, 10^{-6}$. Setting r and α as fixed constants, that is, $r = 2.9$ and $\alpha = 10^{-2}$. The error profiles on the Voronoi polygonal mesh are displayed in Tables 5-6. From these tables, the proposed method still have optimal convergence rate for the velocity and pressure when $\nu = 10^{-2}$. However, as the viscosity decreases, we observe that an increase in the velocity error (from Tables 5) and the proposed method fails to converge even on the finest mesh (from Tables 6). Moreover, the error

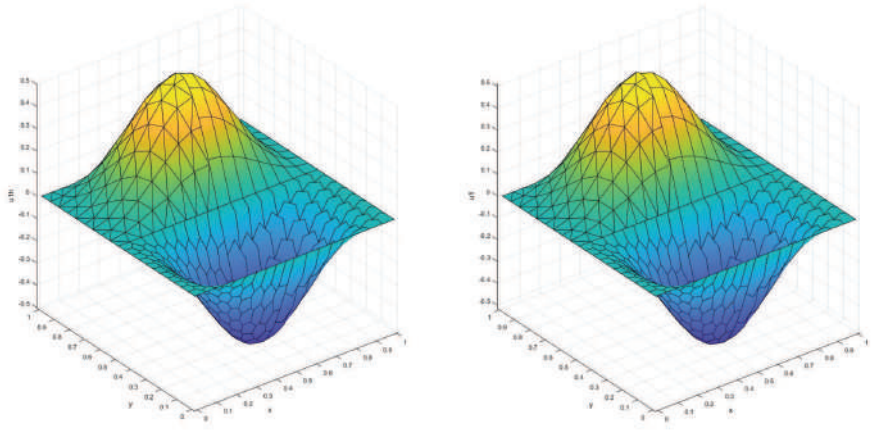

(a) The numerical solution (left) and exact solution (right) of u_1

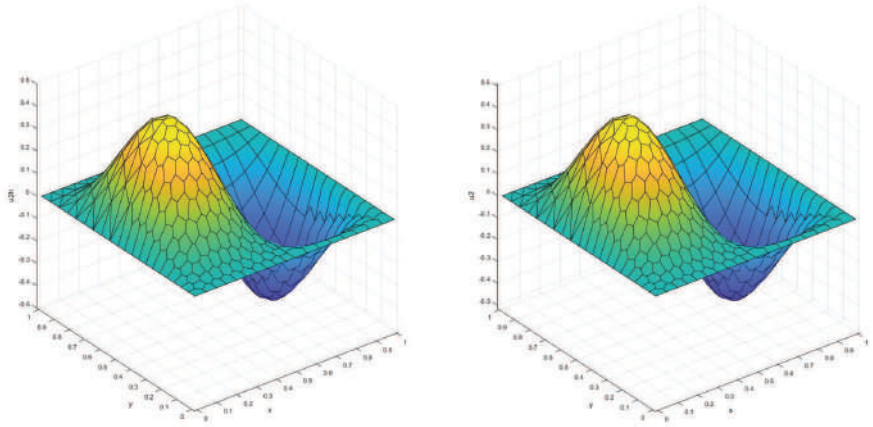

(b) The numerical solution (left) and exact solution (right) of u_2

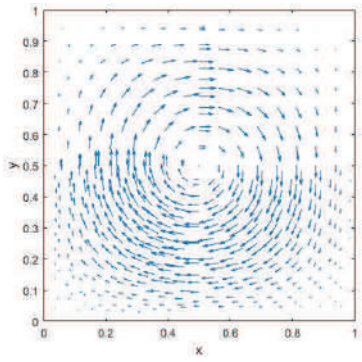

(c) The velocity vector of $\mathbf{u}_h$

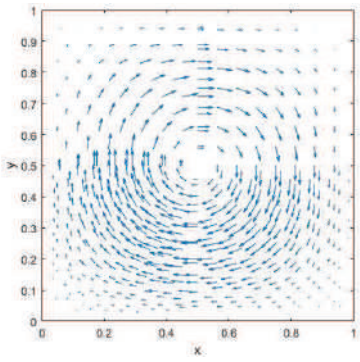

(d) The velocity vector of $\mathbf{u}$

Figure 5: The numerical solution (left) and exact solution (right) are compared in a mixed mesh with 3902 degrees of freedom, using the parameters ν=1e-2, α=1e-2, and r=2.9.

Table 4: The errors for a series of the non-convex meshes $\mathcal{T}^7$ and mixed meshes $\mathcal{T}^8$ on the parameter ν=1e-2, α=1e-2, r=2.9 for Example 6.2.

mesh	# Dof	h	$\mathrm{error}(\mathbf{u}, \boldsymbol{H}^1)$	order	$\mathrm{error}(p, L^2)$	order
$\mathcal{T}^7$	1026	1.250e-01	4.15982e-01	-	2.22504e-02	-
	4098	6.250e-02	7.44477e-02	2.48	6.26340e-03	1.83
	10002	4.000e-02	2.81178e-02	2.18	2.62549e-03	1.95
	20738	2.778e-02	1.32032e-02	2.07	1.27457e-03	1.98
	32402	2.222e-02	8.38221e-03	2.04	8.17000e-04	1.99
$\mathcal{T}^8$	262	1.961e-01	1.22574e+00	-	5.46574e-02	-
	986	1.026e-01	3.19845e-01	2.07	1.70149e-02	1.80
	3902	5.090e-02	6.88956e-02	2.19	5.37271e-03	1.64
	15470	2.534e-02	1.58872e-02	2.10	1.30671e-03	2.03
	61562	1.267e-02	3.82267e-03	2.05	3.38960e-04	1.95

Table 5: The errors for a fixed Voronoi polygonal mesh $\mathcal{T}^6$ on the parameter α=1e-2, r=2.9 and varying values of viscosity ν for Example 6.3.

r,α	viscosity ν	$\mathrm{error}(\mathbf{u}, \boldsymbol{H}^1)$	$\mathrm{error}(p, L^2)$
r = 2.9, α = 1e-2	1e-1	4.87994e-02	4.19320e-03
	1e-2	5.39411e-02	4.12717e-03
	1e-3	1.00950e-01	4.11588e-03
	1e-4	3.05452e-01	4.07627e-03
	1e-5	4.60663e-01	4.07240e-03
	1e-6	4.88016e-01	4.07357e-03

Table 6: The errors for a series of the Voronoi polygonal meshes $\mathcal{T}^6$ on the parameter α=1e-2, r=2.9 and varying values of viscosity ν for Example 6.3.

viscosity	# Dof	h	$\mathrm{error}(\mathbf{u}, \boldsymbol{H}^1)$	order	$\mathrm{error}(p, L^2)$	order
ν = 1e-2	770	1.250e-01	2.52236e-01	-	1.82068e-02	-
	1534	8.839e-02	1.23351e-01	2.06	8.43372e-03	2.22
	3074	6.250e-02	5.39411e-02	2.39	4.12717e-03	2.06
	6134	4.419e-02	2.39696e-02	2.34	2.03280e-03	2.04
	12254	3.125e-02	1.36804e-02	1.62	9.71930e-04	2.13
ν = 1e-4	770	1.250e-01	1.26512e+00	-	1.54389e-02	-
	1534	8.839e-02	9.69139e-01	0.77	7.51311e-03	2.08
	3074	6.250e-02	3.05452e-01	3.33	4.07627e-03	1.76
	6134	4.419e-02	1.47392e-01	2.10	2.05912e-03	1.97
	12254	3.125e-02	1.07834e-01	0.90	9.68447e-04	2.18
ν = 1e-6	770	1.250e-01	1.49533e+00	-	1.49948e-02	-
	1534	8.839e-02	1.47480e+00	0.04	7.19463e-03	2.12
	3074	6.250e-02	4.88016e-01	3.19	4.07357e-03	1.64
	6134	4.419e-02	3.25200e-01	1.17	2.08235e-03	1.94
	12254	3.125e-02	2.73259e-01	0.50	9.76194e-04	2.19

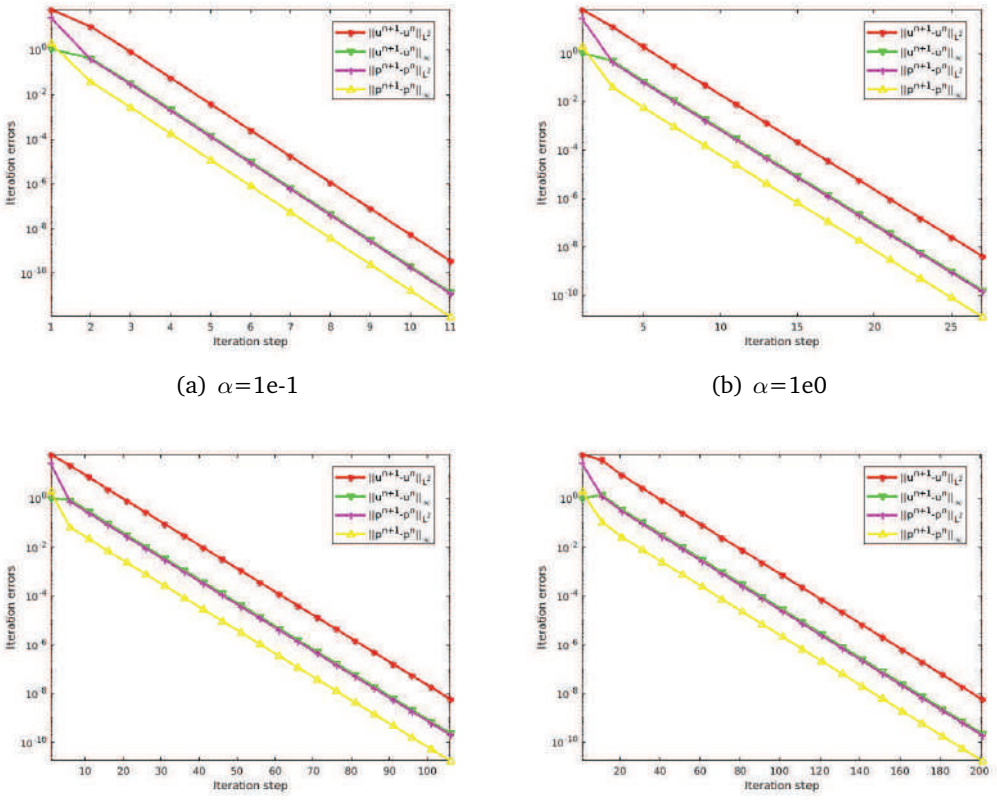

(a) α=1e-1 (b) α=1e0

(c) α=1e1 (d) α=1e2

Figure 6: The iterative errors are compared on a non-convex mesh with different values of the parameter α=1e-1, 1e0, 1e1, 1e2.

of pressure remains almost unchanged with the viscosity decreases. As discussed in the Remark 5.1, due to the lack of pressure-robust [29], the velocity error increases with decreasing values of viscosity coefficient, but the method still is asymptotically pressure approximation for $h \to 0$ (see [29, Remark 3.2]).

Moreover, from the Fig. 6, it is evident that regardless of the chosen parameter configurations, the L^∞-norm error of velocity and the L^2-norm error of pressure consistently exhibit proximity. As the damping coefficient increases, we need to do more iterations for the iterative algorithm to reach convergence.

Example 6.4. Considering a classical lid-driven cavity flow problem [35,38,47], which is called benchmark problem, in a square cavity $\Omega = (0,1) \times (0,1)$. There is no body load, i.e., $\mathbf{f} = 0$. The Dirichlet boundary condition is given as

$$\mathbf{u} = \begin{cases} (1,0)^T, & \text{if} \quad x = 1, \quad y \in (0,1), \\ \mathbf{0}, & \text{otherwise.} \end{cases} \tag{6.4}$$

The Voronoi polygonal mesh $\mathcal{T}^6$ and the mixed mesh $\mathcal{T}^8$ were used in this experiment.

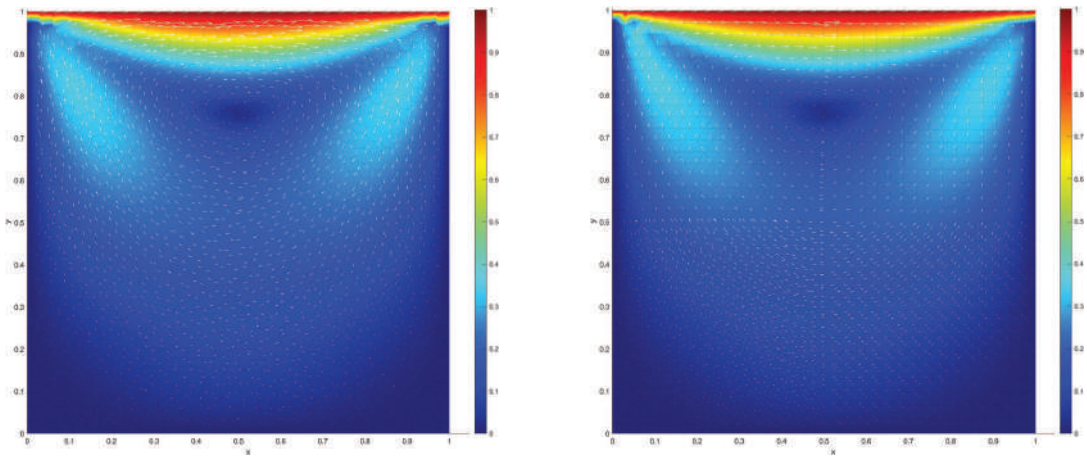

(a) on Voronoi mesh $\mathcal{T}^6$ (b) on mixed mesh $\mathcal{T}^8$

Figure 7: Vectorgraphs and contours of velocity of velocity $\mathbf{u}_h$ in the cavity.

We depicted the vectorgraphs and contours of velocity with $r = 2.9$, $\alpha = 1e-2$, $\nu = 1e-2$ (as shown in Fig. 7). It is evident that under two different mesh configurations, the lid-driven cavity flow problem yields nearly identical velocity distribution results, underscoring the remarkable flexibility of the VEM.

7. Conclusion

This paper explores the application of a divergence-free virtual element method in solving the Stokes equations with nonlinear damping. At the numerical level, this method, characterized by preserving velocity exact divergence-free, ensures mass conservation. By exploiting these properties and topological degree arguments, we proved the well-posedness of the virtual element discretization scheme. Optimal error estimates for velocity and pressure are derived, where

$$\|\mathbf{u} - \mathbf{u}_h\|_{\mathbf{V}} \leq h^s \mathcal{F}(\mathbf{u}; \nu, \alpha_*, \gamma) + Ch^{s+2}|\mathbf{f}|_{s+1}$$

reveals that the error estimate for velocity is explicitly independent of pressure. Numerical experiments have validated the theoretical analysis, demonstrating the stability of the proposed divergence-free virtual element scheme even on various polygonal meshes, including non-convex mesh and mixed mesh with hanging nodes (see Fig. 4). In the third numerical experiment, we analyze the influence of viscosity and damping coefficients on the numerical solution. The experiment revealed a noteworthy phenomenon: the velocity error increases with decreasing values of viscosity ν, but as $h \to 0$, it still exhibits asymptotically pressure-robust [29]. Finally, a classical lid-driven cavity flow problem is studied, once again showcasing the excellent flexibility of the VEM in handing complex domains.

References

[1] B. AHMAD, A. ALSAEDI, F. BREZZI, L. D. MARINI, AND A. RUSSO, *Equivalent projectors for virtual element methods*, Comput. Math. Appl. 66 (2013), 376–391.

[2] S. S. ANTMAN, *The equations for large vibrations of strings*, Amer. Math. Monthly 87 (1980), 359–370.

[3] P. F. ANTONIETTI, L. B. DA VEIGA, AND G. MANZINI, *The Virtual Element Method and Its Applications*, Vol. 31, Springer Nature, 2022.

[4] D. BOFFI ET AL., *Mixed Finite Element Methods and Applications*, Vol. 44, Springer, 2013.

[5] S. C. BRENNER AND L. R. SCOTT, *The Mathematical Theory of Finite Element Methods*, Vol. 3, Springer, 2008.

[6] D. BRESCH AND B. DESJARDINS, *Existence of global weak solutions for a 2D viscous shallow water equations and convergence to the quasi-geostrophic model*, Comm. Math. Phys. 238 (2003), 211–223.

[7] F. BREZZI, R. FALK, AND L. D. MARINI, *Basic principles of mixed virtual element methods*, ESAIM: M2AN 48 (2014), 1227–1240.

[8] X. CAI AND Q. JIU, *Weak and strong solutions for the incompressible Navier-Stokes equations with damping*, J. Math. Anal. Appl. 343 (2008), 799–809.

[9] X. CAI AND L. LEI, *L^2 decay of the incompressible Navier-Stokes equations with damping*, Acta Math. Sci. 30 (2010), 1235–1248.

[10] A. CANGIANI, E. H. GEORGOULIS, AND P. HOUSTON, *hp-version discontinuous Galerkin methods on polygonal and polyhedral meshes*, Math. Models Methods Appl. Sci. 24 (2014), 2009–2041.

[11] L. CHEN, *iFEM: An innovative finite element methods package in Matlab*, University of Maryland, preprint, 2008.

[12] L. CHEN AND F. WANG, *A divergence free weak virtual element method for the Stokes problem on polytopal meshes*, J. Sci. Comput. 78 (2019), 864–886.

[13] A. CHERNOV, C. MARCATI, AND L. MASCOTTO, *$p-$ and $hp-$ virtual elements for the Stokes problem*, Adv. Comput. Math. 47 (2021), Paper No. 24.

[14] A. ÇIBIK, *The effect of a sparse grad-div stabilization on control of stationary Navier-Stokes equations*, J. Math. Anal. Appl. 437 (2016), 613–628.

[15] B. COCKBURN, J. GOPALAKRISHNAN, AND R. LAZAROV, *Unified hybridization of discontinuous Galerkin, mixed, and continuous Galerkin methods for second order elliptic problems*, SIAM J. Numer. Anal. 47 (2009), 1319–1365.

[16] P. CONSTANTIN AND F. RAMOS, *Inviscid limit for damped and driven incompressible Navier-Stokes equations in $\mathbb{R}^2$*, Comm. Math. Phys. 275 (2007), 529–551.

[17] L. B. DA VEIGA, F. BREZZI, A. CANGIANI, G. MANZINI, L. D. MARINI, AND A. RUSSO, *Basic principles of virtual element methods*, Math. Models Methods Appl. Sci. 23 (2013), 199–214.

[18] L. B. DA VEIGA, F. BREZZI, L. D. MARINI, AND R. ALESSANDRO, *H(div) and H(curl)-conforming virtual element methods*, Numer. Math. 133 (2015), 303–332.

[19] L. B. DA VEIGA, F. BREZZI, L. D. MARINI, AND R. ALESSANDRO, *The virtual element method*, Acta Numer. 32 (2023), 123–202.

[20] L. B. DA VEIGA, F. BREZZI, L. D. MARINI, AND A. RUSSO, *The hitchhiker's guide to the virtual element method*, Math. Models Methods Appl. Sci. 24 (2014), 1541–1573.

[21] L. B. DA VEIGA, F. DASSI, AND G. VACCA, *Vorticity-stabilized virtual elements for the Oseen equation*, Math. Models Methods Appl. Sci. 31 (2021), 3009–3052.

[22] L. B. DA VEIGA, C. LOVADINA, AND D. MORA, *A virtual element method for elastic and*

inelastic problems on polytope meshes, Comput. Methods Appl. Mech. Engrg. 295 (2015), 327–346.

[23] L. B. da Veiga, C. Lovadina, and A. Russo, *Stability analysis for the virtual element method*, Math. Models Methods Appl. Sci. 27 (2017), 2557–2594.

[24] L. B. da Veiga, C. Lovadina, and G. Vacca, *Divergence free virtual elements for the Stokes problem on polygonal meshes*, ESAIM: M2AN 51 (2015), 509–535.

[25] L. B. da Veiga, C. Lovadina, and G. Vacca, *Virtual elements for the Navier-Stokes problem on polygonal meshes*, SIAM J. Numer. Anal. 56 (2018), 1210–1242.

[26] K. Deimling, *Nonlinear Functional Analysis*, Courier Corporation, 2010.

[27] D. Di Pietro and A. Ern, *Discrete functional analysis tools for discontinuous Galerkin methods with application to the incompressible Navier-Stokes equations*, Math. Comp. 79 (2010), 1303–1330.

[28] F. Feng, W. Han, and J. Huang, *The virtual element method for an elliptic hemivariational inequality with convex constraint*, Numer. Math. Theor. Meth. Appl. 14 (2021), 589–612.

[29] D. Frerichs-Mihov and C. Merdon, *Divergence-preserving reconstructions on polygons and a really pressure-robust virtual element method for the Stokes problem*, IMA J. Numer. Anal. 42 (2020), 597–619.

[30] M. Frittelli, A. Madzvamuse, and I. Sgura, *The bulk-surface virtual element method for reaction-diffusion PDEs: Analysis and applications*, Commun. Comput. Phys. 33 (2023), 733–763.

[31] V. Georgiev and G. Todorova, *Existence of a solution of the wave equation with nonlinear damping and source terms*, J. Differential Equations 109 (1994), 295–308.

[32] L. Hsiao, *Quasilinear Hyperbolic Systems and Dissipative Mechanisms*, World Scientific, 1997.

[33] X. Huang and F. Wang, *Analysis of divergence free conforming virtual elements for the Brinkman problem*, Math. Models Methods Appl. Sci. 33 (2023), 1245–1280.

[34] Y. Jiang, B. Zheng, and Y. Shang, *A parallel grad-div stabilized finite element algorithm for the Stokes equations with damping*, Comput. Math. Appl. 135 (2023), 171–192.

[35] M. Li, D. Shi, and Y. Dai, *Stabilized low order finite elements for Stokes equations with damping*, J. Math. Anal. Appl. 435 (2016), 646–660.

[36] M. Li, D. Shi, Z. Li, and H. Chen, *Two-level mixed finite element methods for the Navier-Stokes equations with damping*, J. Math. Anal. Appl. 470 (2019), 292–307.

[37] A. Linke and C. Merdon, *Pressure-robustness and discrete Helmholtz projectors in mixed finite element methods for the incompressible Navier-Stokes equations*, Comput. Methods Appl. Mech. Engrg. 311 (2016), 304–326.

[38] D. Liu and K. Li, *Finite element analysis of the Stokes equations with damping*, Math. Numer. Sin. 32 (2010), 433–448.

[39] M. S. Longuet-Higgins, *Theory of weakly damped Stokes waves: A new formulation and its physical interpretation*, J. Fluid Mech. 235 (1992), 319–324.

[40] G. Manzini and A. Mazzia, *Conforming virtual element approximations of the two-dimensional Stokes problem*, Appl. Numer. Math. 181 (2022), 176–203.

[41] L. Mascotto, *The role of stabilization in the virtual element method: A survey*, Comput. Math. Appl. 151 (2023), 244–251.

[42] J. Meng, L. B. da Veiga, and L. Mascotto, *Stability and interpolation properties for Stokes-like virtual element spaces*, J. Sci. Comput. 94 (2023), Paper No. 56.

[43] J. Meng, L. Mei, and M. Fei, *H^1-conforming virtual element method for the Laplacian eigenvalue problem in mixed form*, J. Comput. Appl. Math. 436 (2024), p. 115395.

[44] D. MORA, C. REALES, AND A. SILGADO, *A C^1-virtual element method of high order for the Brinkman equations in stream function formulation with pressure recovery*, IMA J. Numer. Anal. 42 (2021), 3632–3674.
[45] M. OLSHANSKII, G. LUBE, T. HEISTER, AND J. LÖWE, *Grad-div stabilization and subgrid pressure models for the incompressible Navier-Stokes equations*, Comput. Methods Appl. Mech. Engrg. 198 (2009), 3975–3988.
[46] M. OLSHANSKII AND A. REUSKEN, *Grad-div stablilization for Stokes equations*, Math. Comp. 73 (2003), 1699–1718.
[47] H. PENG AND Q. ZHAI, *Weak Galerkin method for the Stokes equations with damping*, Discrete Contin. Dyn. Syst. Ser. B 27 (2022), 1853–1875.
[48] M. RAMMAHA AND T. STREI, *Global existence and nonexistence for nonlinear wave equations with damping and source terms*, Trans. Amer. Math. Soc. 354 (2002), 3621–3637.
[49] N. SUKUMAR AND A. TABARRAEI, *Conforming polygonal finite elements*, Internat. J. Numer. Methods Engrg. 61 (2004), 2045–2066.
[50] C. TALISCHI, G. H. PAULINO, A. PEREIRA, AND I. F. M. D. MENEZES, *Polymesher: A general-purpose mesh generator for polygonal elements written in Matlab*, Struct. Multidiscip. Optim. 45 (2012), 309–328.
[51] G. VACCA, *An H^1-conforming virtual element for Darcy and Brinkman equations*, Math. Models Methods Appl. Sci. 28 (2018), 159–194.
[52] G. WANG, F. WANG, L. CHEN, AND Y. HE, *A divergence free weak virtual element method for the Stokes-Darcy problem on general meshes*, Comput. Methods Appl. Mech. Engrg. 344 (2019), 998–1020.
[53] X. WANG, Q. WANG, AND Z. ZHOU, *A priori error analysis of mixed virtual element methods for optimal control problems governed by Darcy equation*, East Asian J. Appl. Math. 13 (2023), 140–161.
[54] H. WEI, X. HUANG, AND A. LI, *Piecewise divergence-free nonconforming virtual elements for Stokes problem in any dimensions*, SIAM J. Numer. Anal. 59 (2021), 1835–1856.
[55] Y. YU, *mVEM: Matlab programming for virtual element methods*, 2019-2022.
[56] B. ZHANG, J. ZHAO, AND M. LI, *The divergence-free nonconforming virtual element method for the Navier-Stokes problem*, Numer. Methods Partial Differential Equations 39 (2021), 1977–1995.
[57] Y. ZHANG, Y. QIAN, AND L. MEI, *Discontinuous Galerkin methods of the Stokes equations with nonlinear damping term on general meshes*, Comput. Math. Appl. 79 (2020), 2258–2275.
[58] J. ZHAO, B. ZHANG, S. MAO, AND S. CHEN, *The divergence-free nonconforming virtual element for the Stokes problem*, SIAM J. Numer. Anal. 57 (2019), 2730–2759.